Healthcare Analytics 4 (2023) 100261

Contents lists available at ScienceDirect

Healthcare Analytics

journal homepage: www.elsevier.com/locate/health

A systematic review of retinal fundus image segmentation and classification methods using convolutional neural networks

Ademola E. Ilesanmi [a,*], Taiwo Ilesanmi [b], Gbenga A. Gbotoso [c]

[a] University of Pennsylvania, 3710 Hamilton Philadelphia, PA, 19104, United States
[b] National Population Commission, Abuja, Nigeria
[c] Lagos State University of Science and Technology, Ikorodu, Nigeria

ARTICLE INFO

Handling Editor: Madijd Tavana

Keywords:
Convolutional neural network
Retinal fundus
Image segmentation and classification
Eye-related disorders
Retinal disease
Computer-aided image detection

ABSTRACT

Retinal fundus images play a crucial role in the early detection of eye problems, aiding in timely diagnosis and treatment to prevent vision loss or blindness. With advancements in technology, Convolutional Neural Network (CNN) algorithms have emerged as effective tools for recognition, delineation, and classification tasks. This study proposes a comprehensive review of CNN algorithms used for retinal fundus image segmentation and classification. Our review follows a systematic approach, exploring diverse repositories to identify studies employing CNN to segment and classify retinal fundus images. Utilizing CNNs in the segmentation and classification of retinal fundus images can enhance the precision of segmentation outcomes and alleviate the sole dependence on human experts. This approach enables more accurate segmentation results, reducing the burden on human experts. A total of sixty-two studies are included in our review, analyzing aspects such as database usage and the advantages and disadvantages of the methods employed. The review provides valuable insights, limitations, observations, and future directions in the field. Despite certain limitations, the findings indicate that CNN algorithms consistently achieve high accuracies. The comprehensive examination of the included studies sheds light on the potential of CNN in retinal fundus image analysis.

1. Introduction

The prevalence of eye-related diseases has witnessed a significant global increase, leading to a rise in the number of individuals experiencing acute conditions. According to the World Health Organization (WHO), approximately 2.2 billion people worldwide suffer from visual impairment. Alarmingly, around 1 billion cases could have been prevented if timely detection had occurred. In the United States alone, an estimated 40 million people are affected by varying degrees of severe eye-related diseases, with a primary focus on conditions related to the retina, such as glaucoma, among others [1,2]. In Africa, visual impairment affects approximately 26.3 million individuals, with 20.4 million experiencing low vision and 5.9 million being blind, contributing to 15.3% of the global blind population. The leading causes of blindness and visual impairment in this region are uncorrected refractive errors and cataracts. While individuals over the age of 50 are more susceptible to visual impairment and blindness, it is important to note that these conditions can affect people of all age groups. The International Classification of Diseases 11 (2018) categorizes visual impairment into two main groups: 1) Distance vision impairment, ranging from mild to blindness, and 2) Near vision impairment, characterized by acuity worse than N6 or M.08 at 40 cm.

The degree of visual impairment is influenced by several factors, including the availability of preventive measures and treatment options, access to vision rehabilitation services, and the availability of basic amenities such as inclusive buildings, transportation, and information. The leading causes of vision impairment encompass a range of conditions, including: Cataracts, Glaucoma, Diabetic retinopathy, Corneal opacity, Trachoma, Uncorrected refractive error, Age-related macular degeneration. The causes of visual impairment among children can vary depending on the country and social status. In low-income countries, cataracts often emerge as the primary cause, whereas premature retinopathy is a prominent cause in middle-income countries. Uncorrected refractive error remains a leading cause of visual impairment in children across all countries. In the adult population, glaucoma emerges as a significant concern, affecting nearly 80 million people globally and ranking among the leading causes of blindness. Glaucoma can be classified into two main types: open-angle and closed-angle glaucoma.

* Corresponding author.
E-mail address: Ademola.Ilesanmi@Pennmedicine.upenn.edu (A.E. Ilesanmi).

https://doi.org/10.1016/j.health.2023.100261
Received 10 May 2023; Received in revised form 6 August 2023; Accepted 12 September 2023
Available online 22 September 2023

Clinicians estimate that approximately 90% of affected individuals suffer from open-angle glaucoma. Diagnosis of glaucoma involves procedures such as assessing neuroretinal rim loss, conducting visual field tests, and evaluating nerve fiber characteristics [3].

The optic cup, resembling a white cup-like structure at the center of the eye, is positioned within the optic disk. It serves as one of the diagnostic indicators for glaucoma. Diabetic retinopathy (DR) is another prevalent cause of visual impairment, characterized by damage to the tissues located in the blood vessels at the back of the eye. The WHO identifies DR as a significant contributor to blindness, ranking as the fourth leading cause globally [4] (refer to Figs. 2 and 3). In the early stages of DR, there are usually no noticeable symptoms or changes in eyesight. However, if left untreated, it can result in permanent vision impairment. A study conducted by the Center for Disease Control and Prevention in the United States revealed that almost one-third of adults over the age of 40 have DR. Furthermore, over one-third of African-Americans and Mexican-Americans have diabetes, a risk factor for developing DR [5].

Retinal fundus images are photographs that provide a direct optical representation of the eye's internal processes. They capture various morphological and pathological components, including blood vessels, the macula, fovea, optic disk, hemorrhages, arterioles, venules, exudates, and microaneurysms [2]. Fig. 1 illustrates a diagram of retinal fundus images, highlighting different signs of DR, such as exudates, microaneurysms, hemorrhages, and neovascularization.

To prevent visual loss and maintain healthy eyesight, it is advisable to follow the recommendations outlined below: 1) Maintain stable blood sugar levels to minimize the risk of diabetic complications that can affect vision. 2) Be aware of your family's eye health history as certain eye conditions can have a hereditary component. 3) Adopt a balanced and nutritious diet that includes eye-healthy foods to support overall eye health. 4) Maintain a healthy weight, as obesity and excessive weight can increase the risk of various eye diseases. 5) Wear appropriate protective eyewear, such as safety goggles or sunglasses, to shield your eyes from potential injuries and harmful UV rays. 6) Incorporate regular exercise into your routine, as it promotes overall well-being and good blood circulation, which is beneficial for eye health. 7) Reduce or eliminate tobacco usage, as smoking has been linked to several eye diseases and can exacerbate existing visual impairments. 8) Practice proper eye hygiene, including resting your eyes periodically and ensuring clean hands and eye lenses to reduce the risk of infections and other eye-related issues [7–9].

Early detection and diagnosis are crucial in safeguarding against visual impairment and blindness. For individuals with type 1 diabetes, it is recommended to undergo screening for diabetic retinopathy (DR) three to five years after the onset of diabetes, while those with type 2 diabetes should have their first screening within one year of diagnosis [10]. Subsequent examinations should be scheduled every six months or one year, depending on the severity of DR. In cases where the condition is more severe, early and more frequent examinations may be advised. The diagnosis of visual impairment involves a comprehensive examination, including high-quality retinal photography, and a structured follow-up process. Various techniques, such as direct and indirect ophthalmoscopy, stereoscopic retinal fundus photography, and mydriatic and nonmydriatic photographs, are utilized to detect and classify visual impairments.

The gold standard for assessing retinal fundus images is the utilization of stereoscopic photographs in seven standard fields, covering 30° [11–13]. While this approach is accurate and effective, it requires skilled professionals to operate, and the process can be laborious and time-consuming. In many countries, clinicians face a heavy workload due to low doctor-to-patient ratios, leading to potential errors and delays in diagnosis and treatment. As a result, numerous medical photographs taken in hospitals and clinics remain unused and stored within the facilities. Fortunately, these photographs can be valuable resources for Computer-Aided Detection systems (CADs) [14]. CAD systems assist doctors in interpreting medical images by processing digital images and identifying significant areas that may indicate potential disease spots.

Convolutional neural networks (CNNs) have been developed to automatically detect and diagnose ophthalmic issues in retinal fundus images. A notable advantage of CNNs is their ability to learn complex features automatically and translate them into meaningful results. By reducing manual procedures, CNN systems can enhance healthcare practices and serve as a valuable second interpreter. They have the potential to automate eye screening, detect abnormalities, and provide flexibility for healthcare practitioners. The objective of this study is to present the findings of various CNN algorithms used for automatic segmentation, classification, and disease detection in retinal fundus images. This review focuses on recent trends from 2015 onwards, analyzing the performance of different CNN methods, databases, and validation metrics. It also explores the roadmap and challenges associated with CNN detection and diagnosis. Previous research, such as reference [2], has examined deep learning for retinal fundus images, but this review aims to investigate the latest trends, including the pathology and morphologies of retinal fundus images using CNN methods. Additionally, it will address various validation metrics, limitations, and future directions for the segmentation and classification of retinal fundus images. The contributions of this review can be summarized as follows.

1. Analysis of different CNN methods for the segmentation and classification of retinal fundus images, along with an examination of various databases and validation metrics.
2. Discussion of potential challenges and roadmap for CNN utilization in the segmentation and classification of retinal fundus images.

The remainder of the paper is organized as follows: Section 2 provides background information and reviews methods for the

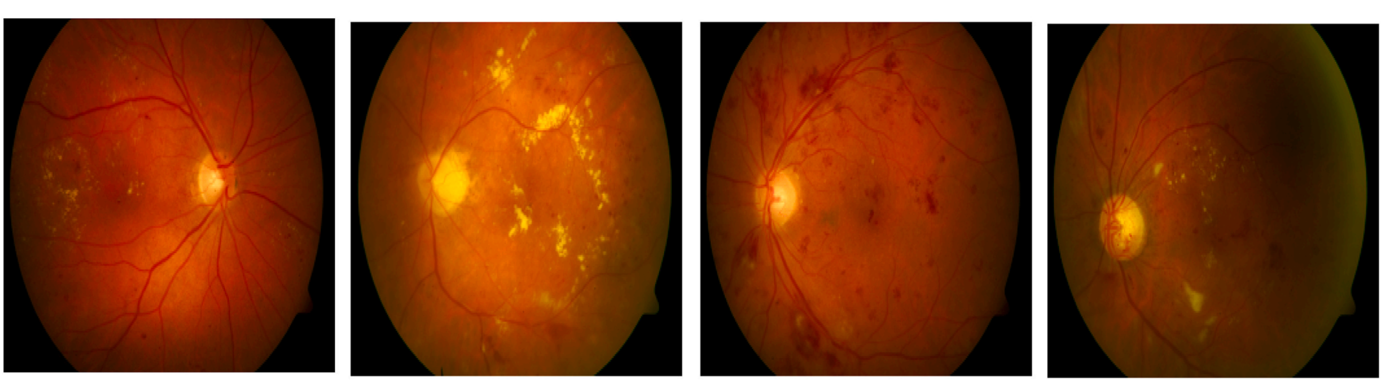

Fig. 1. Retinal fundus images showing different signs of the DR [6].

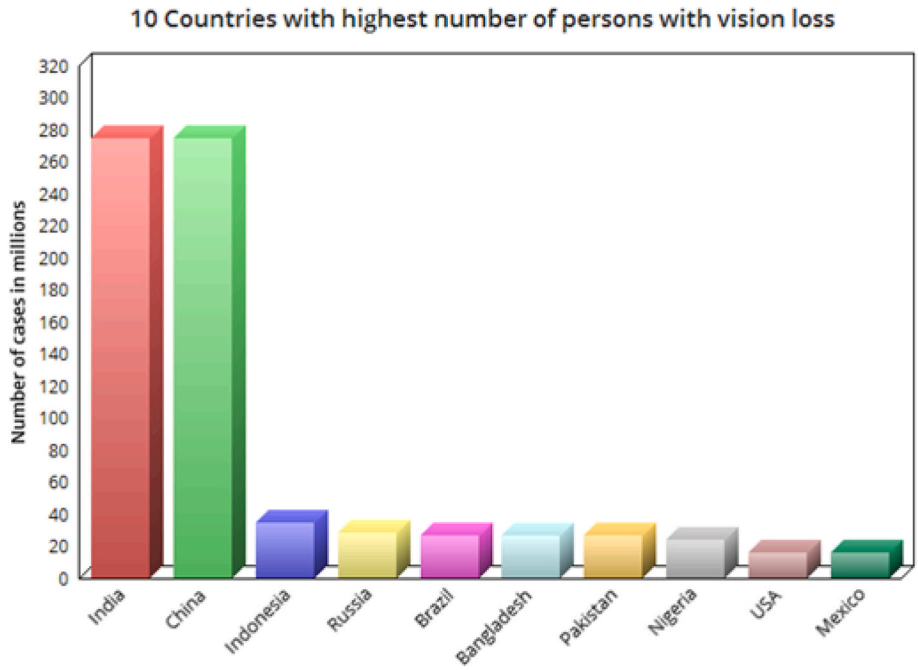

Fig. 2. Cases of vision loss by Countries [1].

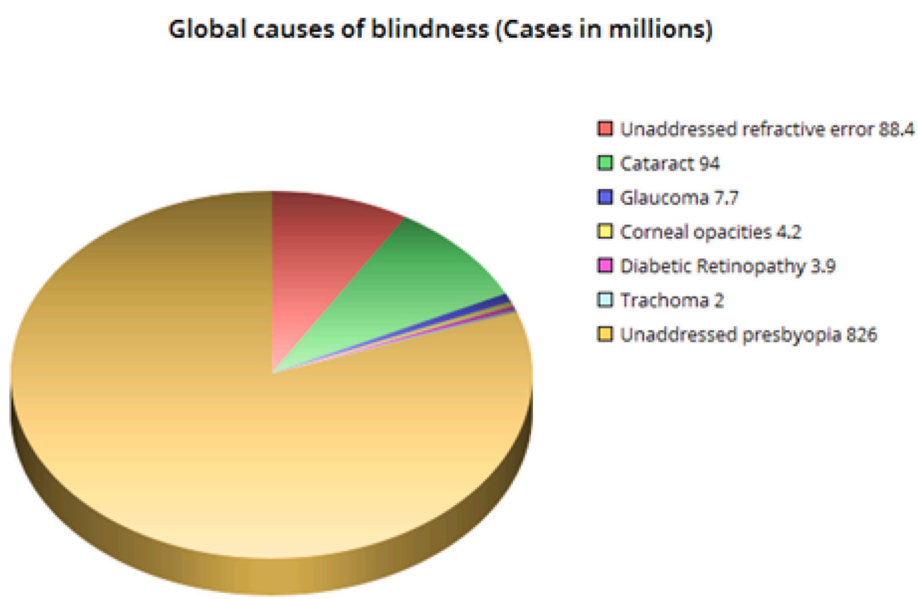

Fig. 3. Global blindness figure [1].

classification and segmentation of fundus images using CNN. Section 3 discusses different evaluation metrics employed in the classification and segmentation processes. Databases are examined in Section 4, while Section 5 presents statistical analyses of different algorithms. Finally, Section 6 concludes the paper.

2. Background

In the 1860s, doctors began exploring potential solutions for capturing images of the eye. By the 1880s, a partial solution had been developed, allowing doctors to take pictures by placing a camera on the patient's head. However, they still had to wait approximately 3 min for the film to develop. Despite its simplicity, this development marked the first time that images of the eye could be captured by anyone. In 1926, the first fundus camera was invented, enabling photography of a portion of the eye. It took another 70 years for the development of a retinal fundus camera capable of capturing images spanning 130°. Eventually, in the 21st century, a non-invasive camera was introduced, capable of capturing a 200-degree view [15].

In the realm of computers, the first algorithm executed on a machine was created by Ada Lovelace in 1843. Since then, numerous algorithms have been developed to perform specific tasks. The field of computer vision emerged in 1966 when computers were employed to identify objects. Mathematical analysis and quantitative applications were introduced to computer vision in the subsequent decade, incorporating techniques such as scale-space representation [16], contour models [17], and Markov random fields [18]. Marvin Minsky's research in mimicking the human brain paved the way for computers to process information for decision-making. In 1959, Russell Kirsch invented a digital image scanner capable of transforming images into digital data. Lawrence Robert processed 3D information about solid objects from 2D photographs in 1963. Kunishiko Fukushima developed the precursor of modern CNNs in 1980. In 1999, David Lowe described a visual recognition system utilizing local invariant features. In 2001, the first real-time face detection framework was introduced.

The breakthrough moment in computer vision occurred in 2012 when AlexNet won the ImageNet competition. Since then, numerous researchers have utilized CNN methods for segmenting and classifying medical images, particularly retinal fundus images. In recent years, the U-shaped Network has emerged as a prominent and effective approach for medical and biomedical image segmentation. Notably, the method introduced by Ronneberger et al. [19] has gained significant recognition. Building upon the U-Shaped architecture, several modifications and variants have been proposed, aiming to further enhance its performance. A comprehensive discussion and exploration of these different U-Shaped variants can be found in Ref. [20].

3. Review of methods

Numerous CNN methods have been proposed by researchers for segmenting and classifying retinal fundus images, employing diverse network architectures to develop sophisticated AI platforms. For instance, Rohit Thanki [21] proposed a CNN method specifically designed to detect glaucoma in fundus images. This approach utilizes a deep neural network for feature extraction and incorporates six machine learning methods for classification. Promising results were obtained, with the logistic regression algorithm achieving the highest classifier accuracy of 0.99 (99%). The method was evaluated on a dataset consisting of 15 normal images and 15 images affected by glaucoma. In another study, Phridviraj et al. [22] proposed a bi-directional Long Short-Term Memory (LSTM) approach for the detection of DR in fundus images. This method employs a three-fold approach. Firstly, a preprocessing technique is applied to enhance the image quality. Secondly, a deep learning-based efficient network is utilized to extract relevant features. Finally, a bi-directional long-term memory classifier comprising six LSTM layers is employed to classify the images. The proposed method achieved an accuracy of 97% when tested on three different datasets.

In the domain of glaucoma classification in fundus images, Kamesh Sonti and Ravindra Dhul [23] proposed a CNN-based approach. Their method consists of 26 layers, including six convolution layers, four pooling layers, and one fully connected layer. A softmax layer is utilized to generate a simple mask prediction for the classifier. Through cross-validation and data augmentation techniques, the method achieved a high-performance accuracy of 96%. In a related study, Raja Sankari et al. [24] focused on detecting retinopathy in fundus images of preterm infants using CNN. Their approach involved preprocessing and segmentation of the images using a modified multiresolution U-Shaped Network [25]. Features were extracted from both traditional methods and deep learning techniques. Subsequently, these features were fed into the random forest algorithm for classification. These research efforts demonstrate the application of CNN in the accurate identification and classification of specific eye conditions, such as glaucoma and retinopathy. The proposed methods showcase the potential of CNN-based approaches in improving diagnosis and treatment decisions based on retinal fundus images.

In this study we emphasize the prowess of CNN methodologies in tackling distinct ophthalmic conditions. Our findings underscore the substantial potential of these techniques for precise diagnosis and effective classification of retinal fundus images. To provide readers with an understanding of the current trends, we have organized these CNN methods into three categories: (1) CNN methods for classifying and segmenting optic discs, (2) CNN methods for classifying and segmenting arteries and veins, and (3) CNN methods for classifying and segmenting retinal blood vessels. Each of these categories comprises a substantial number of CNN methods that have demonstrated promising results. Fig. 4 presents a block diagram illustrating the different CNN approaches, along with a list of prominent CNN methods used within each category.

3.1. *CNN used for segmentation and classification*

3.1.1. *CNN used for optic disk and optic cup*

The automation of optic disk and optic cup segmentation can address challenges encountered in the manual procedure and those anticipated in the future. However, this segmentation technique faces various challenges, including 1) unclear boundaries, 2) significant variability, 3) interference from other image components, and 4) mixed pathologies. To overcome these challenges, researchers have proposed different convolutional neural network (CNN) methods. Wang et al. [26] introduce an encoder-decoder network that consists of two components working in tandem. The first component is the feature detection (FDS) module, which preserves features by employing two stacked convolutional layers (3×3) with batch normalization (BN) and rectified linear unit (ReLU) activations. The second component is the cross-correction sub-network (CCS), which reduces the impact of multiple pooling operations. The decoding block, situated in the second layer of the network, enhances contrast and combines multiple encoding features. In a related study by Fu et al. [27], the segmentation of the optic disc (OD) is accomplished using a combination of the U-shaped network (UNet [19]) and probability bubbles. The images are preprocessed with an iterative robust homomorphic surface filtering method [28].

A two-stage technique aimed at alleviating the class imbalance constraint problem was used by Meng et al. [29]. The candidate's location was determined through a guided search procedure, and a weighted neighborhood voting approach was utilized to generate the localized portable position. Preprocessing of optic disk (OD) and optic cup (OC) images plays a crucial role in medical image processing. This significance is evident in the study conducted by Yuna et al. [30]. In their research, they employed the contrast-limited adaptive histogram equalization (CLAHE) technique [31] for enhancing the image quality before transforming it into polar coordinates [32]. For segmentation purposes, a CNN known as W-Net, comprising feature extractor and context extractor modules, was utilized (refer to Fig. 5 for a clearer visualization).

Due to the intricate connections between structures within the retinal fundus images, the segmentation of candidate regions becomes notably complex. Wang et al. [33] and Tan et al. [34] employed both UNet and a basic CNN for retinal fundus image segmentation. Wang et al. utilized the UNet approach to segment candidate regions within the vessel density map, whereas Tan et al. employed the simple CNN to simultaneously segment and classify three distinct components: vasculature, optic disk (OD), and fovea. The images were normalized and then inputted into the CNN, which consisted of six layers including two convolutional, two max pooling, and two fully connected layers. In order to underscore the significance of preprocessing in retinal fundus images, particularly focusing on the optic disk (OD) and optic cup (OC), Veena et al. [35] employed Gaussian filtering and image normalization techniques to eliminate undesired signals. Global distribution features and the edge histogram texture descriptor (CLAHE and Sobel edge detector [36]) were utilized for structure analysis and detection. The Watershed algorithm [37] was employed to extract contour shapes and localizations. Finally, the end-to-end decoder-encoder method with 39 layers was used. In a different study, Imtiaz et al. [38] introduce a semantic approach that integrates automated augmentation into an encoder-decoder architecture. The encoder block consists of 18 layers comprising 13 convolutions and 5 pooling layers, while the decoder block consists of 20 layers, including 14 convolutions, 5 pooling layers, and 1 softmax layer. For further details, refer to Fig. 6.

In an independent study centered on the utilization of the UNet

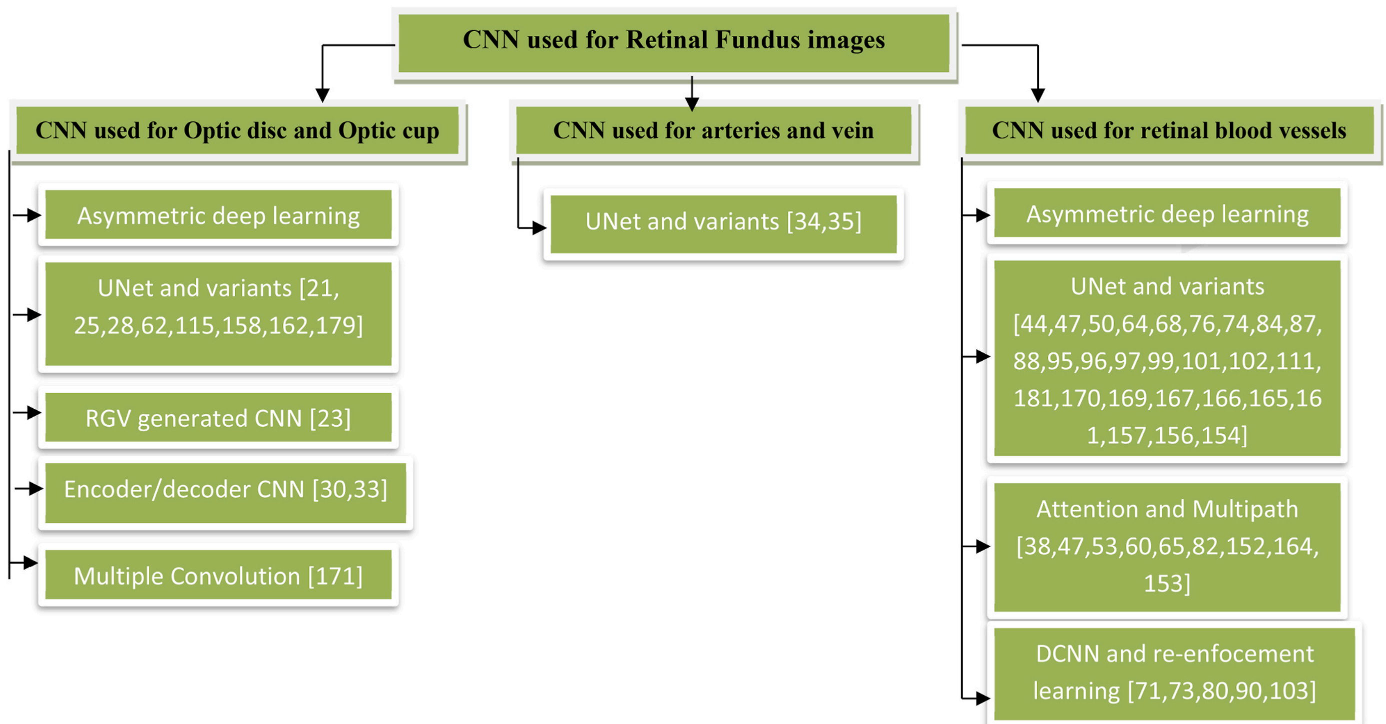

Fig. 4. Categories of CNN methods for retinal fundus images.

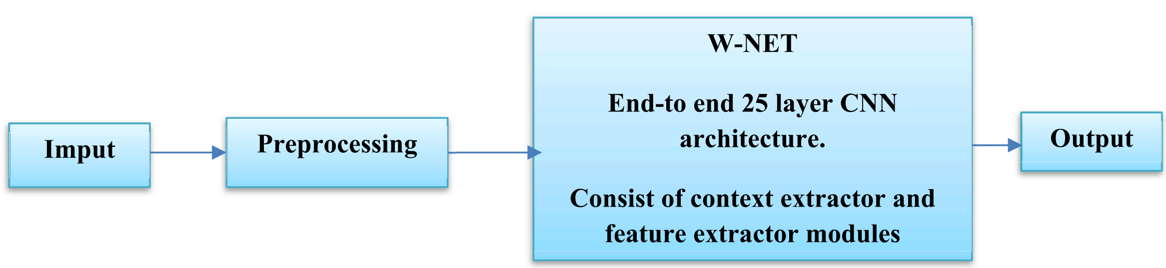

Fig. 5. Multi-scale CNN [30].

model, Xie et al. [39] formulated a coarse-to-fine segmentation approach aimed at establishing an initial segmentation boundary. The CNN methods, specifically a fully convolutional network, were combined with the Viterbi algorithm to segment boundaries. The network consists of three blocks: the encoder, decoder, and sequence decoder. The first two blocks involve traditional encoder and decoder layers, while the sequence encoder layers comprise a gateway module and cascaded gate units. The gateway module receives inputs from each decoder layer and consists of three upsampling and three convolution layers followed by sigmoid activation, while the gate unit comprises ReLU and softmax layers. The Viterbi algorithm [40,41,42] was employed to decode the output of the sequence decoder, modeling the interaction of prediction and spatial constraints. Sadhukhan et al. [43] introduced the attention-based fully connected CNN (AFCNN). This network consists of 19 layers, including three attention blocks, 12 convolution layers, two dropout layers, and one softmax layer. In Priyanka et al. [44], the zero-phase component analysis was applied to the OD image, which was then augmented and fed into the CNN. After being segmented with the CNN, the images were further segmented using the fuzzy c-means method [45]. Similarly, Raja et al. [46] introduced a nine-layer CNN architecture comprising three convolutional layers, four ReLU layers, two max-pooling layers, one fully connected layer, and one softmax layer.

Chowdhury et al. [47] developed a multiscale encoder/decoderguided attention network for multicomponent segmentation of retinal and optic discs. This network incorporates a self-attention mechanism and extracts multiscale features. Hervella et al. [48] introduced a pixel-level and image-level multi-task approach for simultaneously classifying glaucoma and segmenting the optic disc. Gupta et al. [49] employ the U-Net architecture for segmentation and utilize the mayfly optimization kernel extreme learning [50] for classification. Veena et al. [51] developed an enhanced deep learning method for segmenting the optic disc and optic cup. Xiong et al. [52] introduced the Bayesian U-Net Hough transform annotation method, which integrates a Bayesian variant and the copy and crop framework to enhance the weighting of the U-Net. In a different work, Maiti et al. [53] constructed an encoder/decoder network comprising seven subnetworks and integrated a long short-term memory framework. Moreover, multiple other investigations, including Priyanka et al. [44] and Raja et al. [46], employed CNNs for optic disc (OD) segmentation within retinal fundus images. In a recent 2023 study by Rajarshi Bhattacharya et al. [54], an encoder-decoder network was augmented with an auxiliary pyramid decoder. This network features receptive blocks, a modified attention block, and a spatial pyramid network. Notably, promising outcomes were obtained, with dice scores of 94% and 95% achieved for the optic disc and optic cup segmentation, respectively. The study referenced in

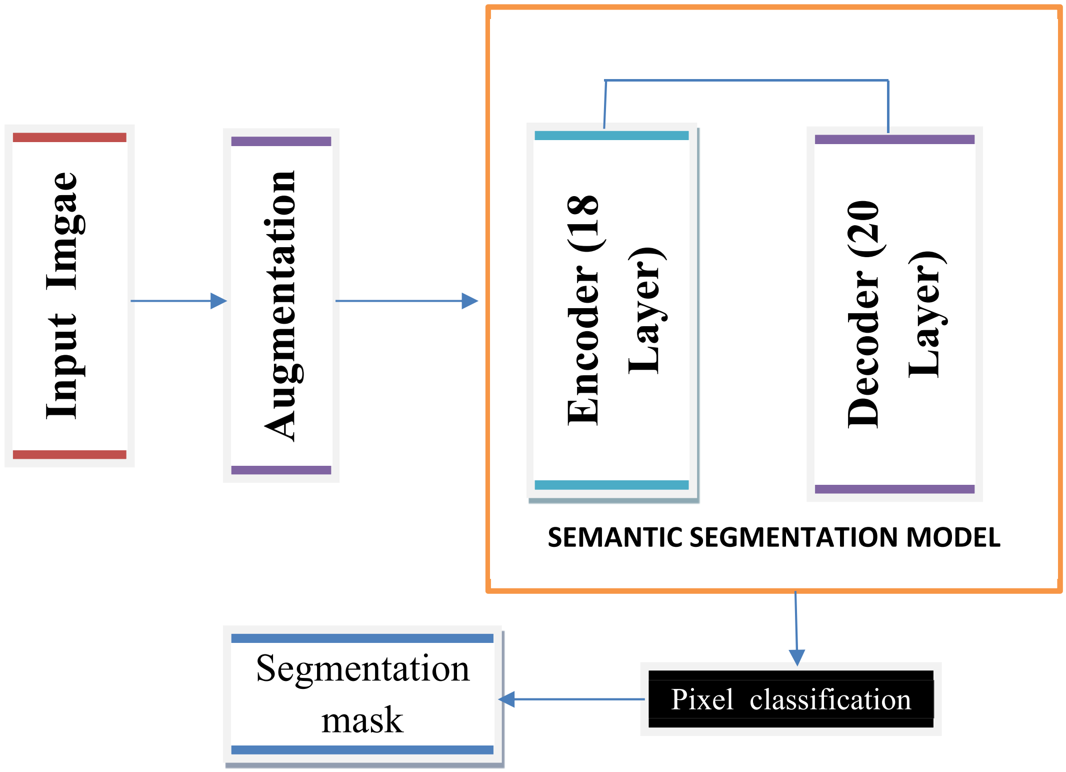

Fig. 6. Label-based semantic segmentation [38].

[55] employed a single-shot multibox detector comprising three key components: a resize module, a feature extractor, and additional feature blocks. A comparison of different methods in this section can be found in Tables 1 and 2.

3.1.2. *CNN used for arteries and vein*

In the study by Girarda et al. [59], they put forth an encoder-decoder CNN model aimed at segmenting arteries and veins. Median filtering was utilized for preprocessing, followed by the stacking of resultant images into the encoder-decoder network. The network comprises 32 feature maps and a final convolutional layer that reduces the map to three classes: background, arteries, and veins. Morano et al. [60] introduced a simultaneous segmentation module inspired by the UNet method. In this study, fundus images were preprocessed with local intensity normalization and channel-wise global contrast enhancement [60]. Subsequently, the UNet was utilized to predict the mask. It is noteworthy that most of the methods employed for arteries and vein segmentation in retinal fundus images are traditional methods, as observed in the available literature. There is a scarcity of CNN-based approaches in this area. For a detailed comparison of different methods in this subsection,

Table 1
CNN used for Optic Disk and Optic Cup.

Author	Ref	Year	CNN Name	Inspiration for research	procedure	Accuracy (Accuracy)
Wan et al.	[26]	2021	Asymmetric deep learning network	UNet [19] M-Net [56]	Segmentation	0.937
Fu et al.	[27]	2021	Fusing UNet with probability bubbles	UNet	Segmentation	0.99
Meng et al.	[29]	2018	RGV generated CNN model	LeNet-5 [57]	Segmentation	0.98
Yuan et al.	[30]	2021	Multi-scale W-Net	M-NET and UNet	Segmentation	0.95
Wang et al.	[33]	2019	Coarse-to-fine deep learning	UNet	Segmentation	0.93
Tan et al.	[34]	2017	Single convolutional neural network	Multiple segmentation	Segmentation	0.96
Veena et al.	[35]	2021	Deep learning enhanced CNN	Encoder-decoder CNN	Segmentation	0.98
Imtiaz et al.	[38]	2021	Label based encoder and decoder semantic segmentation	Encoder-decoder CNN	Segmentation	0.86
Xie et al.	[39]	2020	SU-Net and Viterbi algorithm	UNet, dilated CNN [58], Viterbi algorithm [41,42]	Segmentation	–
Sadhukhan et al.	[43]	2020	AFCNN	FCNN	Segmentation	–
Priyanka et al.	[44]	2017	Patches CNN	CNN, Fuzzy C Means	Segmentation	0.95
Raja et al.	[46]	2020	Traditional CNN	CNN	Segmentation	0.90
Chwodhung et al.	[47]	2022	MGAN	Attention Network	Segmentation	0.91
Hervella et al.	[48]	2022	Multi task method	CNN	Segmentation	0.95
Gupta et al.	[49]	2022	MOKEL	UNet	Segmentation and classification	0.89
Xiog et al.	[52]	2022	Bayesian UNet	UNet	Segmentation	0.94
Maiti et al.	[53]	2022	Multiple convolutions	VGG	Segmentation	0.95
Rajarshi Bhattacharya et al.	[54]	2023	UNet Auxilliary pyramid Network	UNet	Segmentation	0.95

Table 2
Pros and cons of CNN used for Optic Disk and Optic Cup.

Advantages	Disadvantages
Directly training a model using an end-to-end process on both source and target framework. Effortlessly transforms data between different forms. Noise detection is readily achievable due to the superior pixel capture methodology. Images containing fewer symmetrical components are acquired more quickly.	Might exhibit excessive loss. In case of inadequate configuration, it can generate incorrect decoding result. It is simple to overlook crucial features originating from the encoder. Prone to generating deceptive results. Results from symmetric components are notably poor.

please refer to Tables 3 and 4.

3.1.3. CNN used for retinal vessel

Retinal vessel segmentation is a long-standing problem in medical image analysis [61,62], which is accompanied by several challenges, including.

- Presence of various abnormalities of different sizes and shapes: The presence of abnormalities surrounding the vessels in retinal fundus (RF) images can hinder the effective segmentation of vessels.
- Limited availability of annotated data: The scarcity of annotated data can lead to overfitting issues, making it a major challenge when segmenting vessels in FR images.
- Vessel structural differences: Retinal vessels exhibit variations in thickness and structure, making it difficult to find a single model or network suitable for segmenting all types of vessels.
- Unstructured prediction: Pixel classification differs from vessel segmentation, posing challenges in predicting the vessel structure accurately.

To tackle these challenges, several authors have employed CNN methods for vessel segmentation in RF images. Budak et al. [63] introduced the Densely Connected and Concatenated Multi-Encoder-Decoder CNN (DCCMED-CNN). DCCMED utilizes a patch-based learning network and includes both training and testing phases. During training, color patches extracted from raw retina images were used as inputs, and the network weights were trained using stochastic gradient descent methods [64]. The network architecture consists of 2 max-pooling layers, 2 max unpooling layers, 8 concatenated convolution layers, batch normalization, ReLU layers, and a softmax layer. Tang et al. [65] developed the Multi-Proportion Channel Ensemble Model (MPC-EM) for retinal vessel segmentation. MPC-EM comprises 5 submodel networks, with each submodel following an encoder-center-decoder structure. A center architecture is employed as a transitional region to adjust the shape of the feature vector. The subnetworks were optimized using triple convolutional residual blocks to enhance feature extraction and alleviate the vanishing gradient problem [66]. In another approach, Zhao et al. [67] employed a region-based CNN consisting of four parts: 1) backbone for feature extraction, 2) region proposal network, 3) head module for bounding-box regression, and 4) classification for mask generation. The ResNet [68,69] was utilized for backbone feature extraction, and a pyramid structure [70] was adopted to consider multiple scales. The proposed network combined multi-task CNN with 27 layers, 15 convolutional layers, 4 duplicated feature maps, and 2 fully connected layers.

Table 4
Pros and cons of CNN used for Arteries and Vein.

Advantages	Disadvantages
Demonstrates efficacy in preserving edges. Achieves accurate outcomes with a reduced image count.	A low noise ratio can disrupt image edges and generate misleading edge noise, potentially impacting accuracy. Errors might arise during the normalization process. Due to the network's shallowness, exceptional accuracy might not be attainable.

Czepita and Nska [71] employed a shallow UNet architecture for the segmentation of retinal fundus images. The method comprised six stages: 1) Phase image registration: This stage involved aligning the spatial domain of the fundus image to the moving spatial image domain [72]. 2) Vessel probability map generator: The vessel probability stage utilized an encoder-decoder CNN, specifically the shallow UNet model, to extract vessels from the fundus images. 3) Postprocessing: After the initial segmentation, postprocessing techniques were applied to refine the results and improve the accuracy of vessel delineation. 4) Second segmentation: A second round of segmentation was performed to further enhance the quality of vessel segmentation. 5) Region of interest selection: Relevant regions of interest were selected to focus the analysis on specific areas of the retinal image. 6) Vessel diameter measurement: The retinal diameters were measured using a method similar to the one proposed by Ref. [73], specifically the calculation of central venular equivalent (CRVE). Furthermore, Sun et al. [74] presented the multipath cascaded UNet (MCU-Net) for retinal vessel segmentation. The MCU-Net incorporated three types of data as input: raw FFA, small-scale FFA, and large-scale FFA. The network fused vessel features from these inputs to generate a vascular probability map as the output. It comprised an attention gate [75] in conjunction with a residual recurrent unit [76]. The MCU-Net encompassed two specific blocks: the refinement block and the FFA image fusion block. For a more detailed understanding, please refer to Fig. 7.

As evident from various studies, numerous researchers have employed the UNet architecture RF segmentation. The UNet was employed either in its original configuration or with adaptations to the original structure. An illustration of such a modification can be found in the work of Zhao et al. [69], who introduced the Nested U-shaped attention network (NUA-Net) for segmenting and classifying retinal images. The image was first enhanced thereafter, the green channel images were used as the network inputs (the same as the methods in Ref. [77]). The NUA-Net has an encoder stage and each encoder stage has a 2 × 2 max-pooling followed by convolution with batch normalization, ReLU, and dropout. Guo et al. [78] proposed the multiscale deeply supervised network with short connection (BTS-DSN). This network used short connections to transfer semantic information between side-output layers. Two approaches were considered: the bottom-top short connections and the top-bottom short connections. The key element of this network is the top-bottom, and bottom-top short connection approaches. A switch of connectivity within layers gives the BTS-DSN a flexible procedure. Guo et al. [79] proposed the multiple deep convolutional neural network (MDCNN) for a formulated classification and segmentation task. The MDCNN was constructed by cascading multiple networks with the same structure.

Noh et al. [60] proposed the scale-space approximation for multi-scale representation in CNN (SSANet). The SSANet consists of 3

Table 3
CNN used for Arteries and Vein.

Author	Ref	Year	CNN Name	Inspiration for research	procedure	Accuracy
Girard et al.	[59]	2019	Joint segmentation model	UNET	Segmentation	0.96
Morano et al.	[60]	2021	Simultaneous segmentation	UNET	Segmentation	0.96

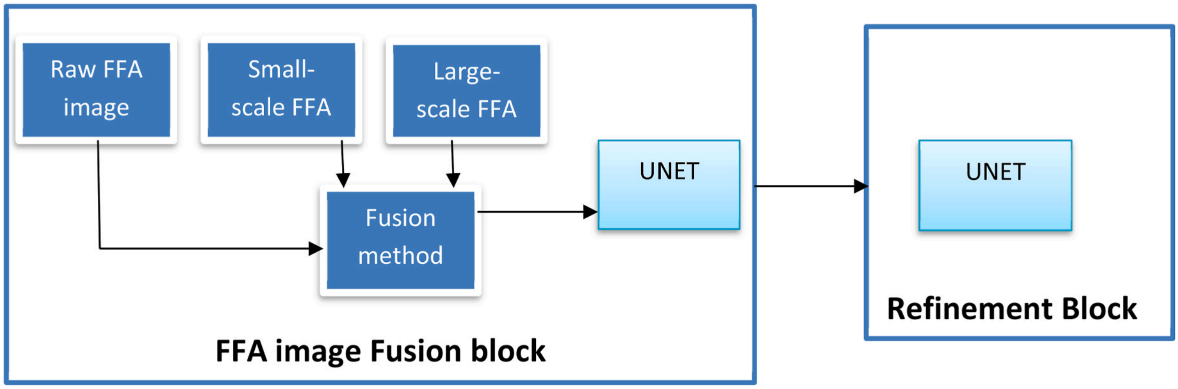

Fig. 7. MCU-net [74].

blocks, (feature generation, feature aggregation, and inference) with 33 layers. The feature generation block has 21 layers consisting of 1 convolution layer, 3 upsampling layers, and 17 ResBlock layers. The aggregation stage perform two key procedure: it moves input before each upsampling in the generation block. Secondly, it accepts inputs from the final block of the generation using 9 layers (5 Convolutional layers, and 4 upsampling layers). The inference block collects inputs from the aggregation and transforms these inputs to a mask. Zhuo et al. [80] combined the size-invariant feature maps [81] with the dense connectivity [82] (SID^2Net) for the segmentation and classification of RF. The SID^2Net has two bottleneck modules, three dense blocks, two convolutional layers and a sigmoid layer for prediction. An ablation experiment was carried out dividing the network into the dense network (DNet), and DNet with size-invariant feature maps (SIDNet). Hervella et al. [83] used the multi-instance heating regression to predict RF image segmentation. This method predicts binary maps with the pixels corresponding to the location and labeling of the positive class of the ground truth. The RF images were passed to the UNET framework and the results were interpolated back into the original RF images.

The skip-chain convolutional network is a model design integrating skip connections or shortcuts among layers, aiming to amplify information flow and improve feature acquisition. For the specific task of blood vessel segmentation, a vessel-specific skip-chain convolutional network (VSSC Net) developed by Samuel et al. was employed. The VSSC Net operates through two stages: preprocessing and segmentation. The preprocessing stage converts RF images to grayscale then the adaptive fractional difference approach [84] followed by the CLAHE is applied to the grayscale image. The segmentation stage (VSSC Net) is an end-to-end framework that takes input images of arbitrary size producing a probability map. VSSC Net has two components: base network architecture and novel architecture. The base network consists of different convolutional layers split into 4 pairs. The visual geometry group (VGG-16) [85] was used as the base network. The attention-based before-activation residual UNet (BSEResU-Net) [86] exploits the attention mechanism and the dropblock regularization method to reduce overfitting. The images were preprocessed by transforming RGB images to grayscale, and the CLAHE algorithm was applied to the grayscale image. The ResU-Net has 33 convolutional layers with 16 residual operations, 2 transpose convolutional layers, 2 downsampling layers, and 1 output map. Huang et al. [87] proposed the multipath scale network (MPS-Net) for retinal vessel segmentation. The MPS-Net is an end-to-end network that uses one high-resolution RF input and produces a probability map with two low resolutions as output. The network has 13 multi-path scale modules, 3 convolution + ReLU, 3 Normalization + ReLU, and 1 cropping layer. The multi-path scale module has 3 regional paths concatenated together and arranged horizontally to produce the output. The range entropy [88] definition was introduced to describe vessel information of the feature maps.

Tian et al. [89] proposed the multipath CNN for RF segmentation. This network converts the original image to low-frequency and high-frequency images with the low-pass Gaussian filter and the high-pass Gaussian filter. The CNN consists of a convolution down-sampling and convolution upsampling and has 32 convolutional layers with four blocks of 64, 128, 64, and 32. Ultimately, the outcomes of the initial and secondary CNN were merged (fused) together to generate the conclusive segmentation result. To find out if there is a difference between the preprocessed image and the images without preprocessing, Atli and Gedik [90] used the Sin-Net for the segmentation of vessels in RF images. To preprocess, the CLAHE and the multi-scale top hat transform (MTHT) [91] were used to enhance image contrast. The Sin-Net architecture consists of 17 layers comprising 11 convolution operations, 2 upsampling layers, 2 down-sampling layers, 1 output and input layer each.

The usage of reinforcement learning in RF images is gaining prominence. Guo et al. [92] used CNN with reinforcement learning to segment vessels in RF images. The images are divided into smaller patches and sent to CNN for training. The CNN has five components: convolution, pooling, dropout, fully connected, and loss function. Deep CNN [93] has received tremendous recognition in medical image processing. As an example, Wu et al. [94] introduced the Network Followed Network (NFN+), which encompasses four distinct modules: 1) encoder and decoder of the initial network, 2) encoder and decoder of the subsequent network, 3) front group of intra-network skip connections, and 4) second group of inter-network skip connections. In summary, the NFN + architecture incorporates two connections involving the front and followed networks, encompassing a total of 10 integrated components, including convolutions, batch normalization, and dropout layers. Fully convolutional networks (FCN) have gained relevance in tasks related to nonmedical imaging. However, such tides are changing, Hemelings et al. [95] used the FCN for segmenting retinal vessels in RF images. They used the method adopted by Ref. [96] to pad the region of interest to avoid excessive contrast enhancement at the border of the image. The CLAHE, and noise removal methods were used to preprocess the RF and passed to network architecture for segmentation. Boudegga et al. [97] proposed RV-Net for vessel segmentation. This method preprocesses the RF images by replacing the black area with an average color (see Ref. [98]), then the image was converted to LAB. The CLAHE algorithm is applied to the image and the channels are merged and converted back to RGB. The preprocessed image was augmented by performing image transformation, cropping, and patch extraction [99]. The images were fed into the network for segmentation by the RV-Net. Wang et al. [100] proposed the hybrid CNN and ensemble random forest (RFs) [101] method. CNN was used for segmentation while the RF was the trainable traditional method used for classification. The CNN has 5 layers consisting of the convolution, subsampling, and fully connected layer. Hu et al. [102] conducted a study introducing a multiscale CNN with a cross-entropy loss function for retinal vessel segmentation. The original RF image underwent augmentation before being fed into the network.

The multiscale CNN framework comprised four distinct stages. The first and second stages comprised four convolutional layers and one max-pooling layer each. At the beginning of the network, there were a total of 20 convolutional layers and three max-pooling layers. For a more comprehensive understanding, please refer to Fig. 8.

Zhou et al. [103] proposed the symmetric equilibrium generative adversarial network (SEGAN) for vessel segmentation. The SEGAN is an end-to-end synthetic neural network that utilizes the adversarial principle. Three fundamental principles were employed in this study: SEGAN, multiscale feature refine block (MSFRB), and attention mechanism (AM) [104]. Overall, there were 13 traditional layers, 5 MSFRB, and 5 a.m. layers. The research by Ref. [105] proposed a hybrid multitask deep learning for segmenting vessels. The original image was annotated before being fed into the deep learning algorithm. The network has two modules: 1) multitask segmentation, 2) fusion network module. For both modules, the improved UNet framework was adopted for segmentation and fusion. The network is an encoder-decoder segmentation consisting of 20 layers. The output of the segmentation was passed to the fusion layer for the final output. The deformable U-Net (DUNet) proposed by Jin et al. [106] is a U-shaped architecture with an encoder and decoder framework. Some of the convolutional layers in the traditional UNet were replaced with deformable convolutional blocks. The DUNet integrates the low-level features with high-level features. The design was constructed with 4 convolution layers, 4 batch normalizations, and 4 ReLU layers. Soomro et al. [107] proposed the strided fully connected CNN for the segmentation of vessels in RF images. The images were preprocessed with morphological tactics and the principal component analysis (PCA) [108]. The network has 5 fully consecutive convolutional blocks with sizes ranging from 16, 32, 64,128, and 256 features. There is no ablation experiment in this research.

Chala et al. [109] proposed the end-to-end improved CNN for vessel segmentation. This network used the multi-encoder-decoder principle and a new progressive reduction model that was integrated into the network. The network has 4 interconnected components (multi-encoder and parallel components, RGB-encoder and green channel encoder, decoder component, and progressive reduction components). Data augmentation was performed to generate more data for the network. Sun et al. [110] proposed the contextual information enhanced UNet (CIEU-Net) with dilated convolutional module for vessel segmentation. The cascaded dilated module and the pyramid module were integrated to form the segmentation network. Wu et al. [111] proposed the scale and context-sensitive network for the segmentation of vessels. The model consists of three modules: scale-aware feature aggregation (SFA), adaptive feature fusion (AFF), and multi-level semantic supervision (MSS). The SFA adjusts the receptive field dynamically to extract features. The AFF guides the fusion between features efficiently. Sathananthavathi and Indumathi [112] proposed the enhanced encoder atrous UNet (EEA-UNet) for retinal vessel segmentation. The images were preprocessed with the CLAHE and resized to 512 × 512. Post-processing was done by morphological operations to remove isolated false positives. The EEA-UNet is an asymmetric contraction and expansion path that replaces all the convolutions as the atrous convolution to increase the receptive field. The contracting has 5 blocks containing 2 atrous convolutions, batch normalization, pooling, and ReLU layer. The atrous convolution reduces the image size without losing the significant features in it [113].

Yin et al. [114] proposed a U-shaped deep learning fusion network (DF-Net) for vessel image segmentation. The method involves 4 stages: multiscale fusion, U-shaped network, feature fusion, and classifier fusion. The original image was multiscaled by the image pyramid [115] and constructed on a multiscale input integrated into the encoder path for information fusion. The encoder of the network encompasses 2 convolution layers, coupled with max-pooling employing ReLU activation. The decoder, on the other hand, entails 2 convolutional layers, succeeded by up-sampling with the number of feature maps halved. The vessel fusion module is attached to the decoder and enhanced with the corresponding output features. This network is combined with the Frangi filter and a deep neural network was trained. The research by Tang et al. [116] adopts the multiscale method. The authors developed multi-scale channel importance sorting (MSCS) for vessel segmentation. First, the CLAHE algorithm was used to enhance the image before it was fed to the network. The MSCS is an encoder-decoder that consists of 3 encoders and 2 decoder blocks. Each encoder block consists of multi-scale, channel importance, and a convolution layer. Between the encoder and decoder, the spatial attention mechanism was used instead of the traditional skip connection to read the output and characterize the encoder generating the attention coefficients. The research by Ref. [117] proposed the cascaded attention residual network (AReN-UNet). The AReN-UNet features a unique aggregated residual module, which incorporates concatenated max and average pooling, along with a shared multilayer perceptron (MLP) [118] concluded with a sigmoid layer. Shi et al. [119] developed the multiscale dense network (MD-Net) that makes good use of the multi-scale features and the encoder features. This network is preprocessed with the CLAHE algorithm. A residual atrous spatial pyramid pooling (Res-ASPP) was blended into the error framework and the dense multi-level fusion merges the features in the encoder and decoder. A squeeze and extraction (SE) block was applied to the concatenated layer for effective feature channels. The Res-ASPP has 12 layers all of which are convolution layers with varying dimensions and sizes. The multi-level fusion mechanism and SE block perform the fusion procedure in the network.

Tchinda et al. [120,121] used the combination of edge detection and neural network to segment vessels in RF images. The method used feature vectors with eight characteristic pixels. The feature vectors include 1) image gradient obtained with edge detection (Prewitt, Sobel, Canny, and Gaussian [122,and123]]), 2) the Laplacian of Gaussian filter, 3) morphological transformation (erosion, dilation, and top hat filtering [124]). The cascaded feed-forward network was used for segmentation. Gegundez-Arias et al. [125] proposed the simplified UNet for the segmentation of RF images. A combination of the residual block and batch normalization in the upsampling and downsampling layers produces the required segmentation results. The simplified UNet has 10 blocks consisting of 1 CONV_ReLU1 layer, 1 convolution layer, 3 Block2 layers, 2 Block I1, and 3 Block I2 layers. Skip connections were used to link Block I1 and Block I2 together. Maji et al. [126] combined the attention-based neural network with transfer learning. This research

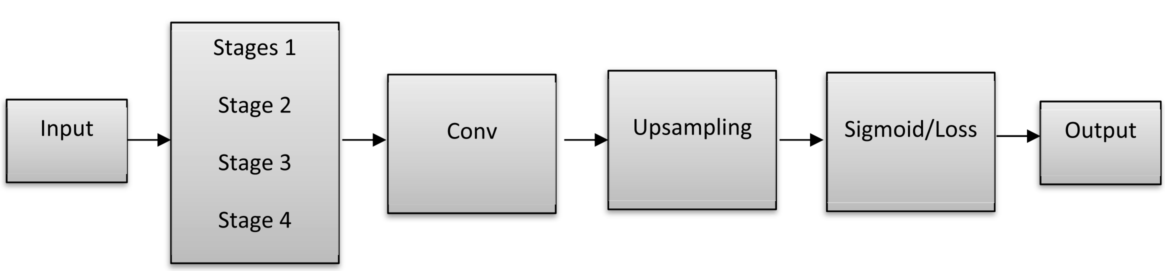

Fig. 8. Multiscale CNN [102].

used the optimized learning method to classify and grade RF images. The attention mechanism adds attention to pixels near the vessel. The Gaussian filter was used to normalize color balance and illumination, then the data was augmented. The softmax graded the health risk with 0 as bad and 2 as good. Sangeethaa and Maheswari [127] used morphological process, thresholding, edge detection, and adaptive histogram for segmentation, while CNN was used for classification. After preprocessing and segmentation, the image was fed into the trained CNN for classification (either normal or diseased).

Muthusamy et al. [128] used the CNN recurrent network (CNN-RRN) to segment retinal images. The image was first preprocessed with the median filter for denoising and smoothing. Then, the image was resized with dual-tree complex wavelet transform and then the classification was done using renewal networks (CNN with recurrent neural network concept [129]). Shi et al. [130] developed a graph-based convolutional feature aggregation network for segmenting retinal vessels. The model consists of multilevel feature extraction, and a graph-based high and low aggregation model. In this network, features are extracted at different levels and passed to high and low aggregation models for preprocessing and segmentation. Song Guo [131] proposed the cascaded guided network for retinal vessel segmentation. This network consists of three branches each with a scale of different sizes. Each of the branches consists of connected multiscale multidirectional feature learning modules to learn under the low-resolution feature and segments semantic maps as output. Ren et al. [132], combined the U-Net network and the BiFPN [133] for the segmentation of retinal vessel images. This network is an encoder-decoder network and the BiFPN was used as the skip between the encoder and decoder. Hang et al. [134], proposed the improved U-Net with the skip layer replaced with a multilayer connection (NOLnet). The NOL block consists of transpose convolutions, batch normalization, and concatenation layers. Xu & Fan [135] proposed the dual-channel asymmetric convolution neural network. This network consists of two parts (mainsegment Net and Finsesegment Net). The original image was divided into two thick feature maps, with each feature map used as input to the two networks.

Zhong et al. [136]; developed a multiscale dilated convolutional neural network (MMDC-Net) to capture information from receptive fields. They perform a cascading procedure on the U-Net and used a multilayer fusion (MLF) model to fuse features and filter noise. A width attention CNN (WA_net) proposed by Ref. [137] for retinal vessel segmentation was used to decompose multiple channels of feature maps into categories. Deng & Ye [138] proposed a multi-scale attention mechanism residual deformable convolution that combines the M-shaped network with the pulse-coupled neural network. Similarly, Huang et al. [139], proposed the cascaded self-attention U-shaped network. The network used the U-Net and the residual self-attention model to segment retinal fundus images. The network progressed from fine to coarse segmentation before producing the final mask. Pavani et al. [140], proposed the multistage dual-path interactive refinement network. This network follows a single encoder and dual decoder style. Data augmentation with model implementation was used to boost the network. Karlsson & Hardarson [141] proposed a CNN based on several interconnected U-Nets. The network was simultaneously connected and sandwiched with global features and exceptional linear units [142]. Zhu et al. [143], proposed an inception-based U-Net that consists of two parts: inception downsampling (connected to the encoder) and inception upsampling (connected to the decoder). A copy framework was added to the decoder to help refine the network. The network proposed by Yin et al. [144], used the U-Net, feature fusion, and classification fusion network. The network was a multiscale network used to fuse all features after segmentation. The segmentation outputs from each encoder were downscaled and combined to yield the final outcome.

Khan et al. [145] introduced a novel approach called the multi-resolution contextual network for the segmentation of vessels in RF. This network leverages multiscale features to capture contextual dependencies through a bi-directional context learning framework. Liu et al. [146] conducted a study utilizing the dual attention Res2Unet (DA-Res2UNet) for retinal vessel segmentation. In this method, the convolution layer in the traditional UNet was replaced with the Res2-Block and a DropBlock. The spatial attention and dual attention mechanisms were key components of this approach. Comparative analysis demonstrated a segmentation accuracy of 97% when compared to other state-of-the-art methods. In a separate study, Liu et al. [147] proposed the attention augmented Wasserstein generative adversarial network (AA-WIGAN) for retinal vessel segmentation. The network employed an advanced UNet as the generator and a discriminator. Experimental results exhibited promising outcomes with a segmentation accuracy of 97%. For further details and a comprehensive comparison of different methods, please refer to Tables 5 and 6.

4. Performance measures

The evaluation metrics used to assess the performance of various CNN methods in the segmentation and classification of retina fundus images include the following.

1) True Positive (TP): The number of correctly identified positive instances or correctly segmented/classified abnormalities in the image.
2) False Positive (FP): The number of incorrectly identified positive instances or incorrectly segmented/classified abnormalities in the image.
3) False Negative (FN): The number of incorrectly missed positive instances or incorrectly unsegmented/unclassified abnormalities in the image.
4) True Negative (TN): The number of correctly identified negative instances or correctly classified background/non-abnormal regions in the image.
5) Intersection over union (IOU): measures the degree of overlap between the ground truth (GT) and the segmented prediction, quantifying it within a range of 0–1. This overlap assessment, commonly referred to as the Intersection over Union (IOU), is also synonymous with the Jaccard index.

$$IOU = \frac{GT \cap Prediction}{GT \cup Prediction} \tag{1}$$

6) Recall: this method characterizes the relevant portion of the positive segmentation prediction in relation to the ground truth. It aligns with the concept of sensitivity, indicating the proportion of positive cases accurately classified by the method.

$$Recall = \frac{Tp}{Tp + Fn} \tag{2}$$

7) Precision: This metric quantifies the positive predictions in relation to the ground truth.

$$Precision = \frac{Tp}{Tp + Fp} \tag{3}$$

8) Accuracy (ACC): This measurement computes the sum of true positive and true negative, divided by the total number of positives and negatives.

$$ACC = \frac{Tp + Tn}{Tp + Tn + Fp + Fn} \tag{4}$$

Table 5
CNN used for Retinal vessel.

Author	Ref	Year	CNN Name	Inspiration for research	procedure
Budak et al.	[63]	2020	Densely connected/concatenated multi-encoder-decoder CNN	Feedforward CNN	Segmentation
Tang et al.	[65]	2019	Multi-proportion channel ensemble model	Ensemble model	Segmentation
Zhao et al.	[67]	2020	RCNN-based junction refinement network	Masked RCNN-model [148]	Segmentation
Yuan et al.	[71]	2021	Shallow U-Net	UNet	Segmentation
Sun et al.	[74]	2021	Multi-path cascaded UNet	UNet	Segmentation,
Zhao et al.	[69]	2021	Nested U-shaped attention network	UNet	Segmentation
Guo et al.	[78]	2019	Bottom-top and top-bottom short connection deep supervised network	Deep supervised network	Segmentation
Guo et al.	[79]	2018	Multiple deep CNN	Deep CNN [149]	Segmentation
Noh et al.	[150]	2019	Scale-space approximated CNN	DRIU [151]	Segmentation
Zhuo et al.	[80]	2020	Size-invariant and dense connectivity network	DenseNet Network [82]	Segmentation
Hervella et al.	[83]	2020	Multi-instance heat map regression	DNN	Segmentation
P. M Samuel & T. Veeramalai	[152]	2021	Vessel Specific Skip chain CNN	Fully convolutional networks	Segmentation
D. Li & S. Rahardja	[86]	2021	Attention-based before-activation residual U-Net	Modified UNet	Segmentation
Lin et al.	[87]	2021	Multi-path scale network	HR-Net [153]	Segmentation
Tian et al.	[89]	2020	Multi-path CNN	UNet	Segmentation
I. Atli & O. S. Gedik	[90]	2021	Sine-Net CNN	Fully CNN	Segmentation
Guo et al.	[92]	2018	CNN with reinforcement sample learning.	Reinforcement learning	Segmentation
Wu et al.	[94]	2020	A network followed network.	Deep CNN [93]	Segmentation
Hemelings et al.	[95]	2019	Fully convolutional network.	UNet	Segmentation
Boudegga et al.	[97]	2021	RV-Net	UNet, AlexNet [154], VGG	Segmentation
Wang et al.	[100]	2015	Features and ensemble learning	CNN, and RFs	Segmentation and classification
Hu et al.	[102]	2018	Multiscale CNN	Richer convolutional features [155]	Segmentation
Zhou et al.	[103]	2021	Equilibrium GAN	UNet, GAN [156]	Segmentation
Yang et al.	[105]	2021	Improved UNet	UNet	Segmentation
Jin et al.	[106]	2019	DUNet	UNet, Deformable convNet [157]	Segmentation
Soomro et al.	[107]	2019	Strided FCNN	SegNet [158]	Segmentation
Chala et al.	[109]	2021	Improved deep CNN	DCNN	Segmentation
Sun et al.	[110]	2021	CIEU-Net	UNet	Segmentation
Wu et al.	[111]	2021	SCS-Net	UNet	Segmentation
Sathananthavathi & Indumathi	[112]	2021	EEA UNet	UNet	Segmentation
Yin et al.	[114]	2021	DF-Net	UNet	Segmentation
Tang et al.	[116]	2020	MSCS	UNet	Segmentation
Rahman et al.	[117]	2021	Cascaded AReN-UNet	UNet	Segmentation
Shi et al.	[119]	2021	MD-Net	SegNet, PSPNet [159], UNet	Segmentation
Tchinda et al.	[120]	2021	Classical edge detection and neural network	Artificial neural network	Segmentation
Gegundez-Arias et al.	[125]	2021	Simplified UNet	UNet	Segmentation
Maji & Sekh	[126]	2020	Tradition method with CNN	CNN	Classification
Sangeethaa & Maheswari	[127]	2018	Trained CNN	CNN	Segmentation and Classification
Muthusamy & Tholkapiyan	[128]	2019	CNN-RNN	CNN	Segmentation and Classification
Shi et al.	[130]	2022	Graph-based network	Multilevel method	Segmentation
Guo	[131]	2022	Cascade guided network	Multiscale method	Multiscale methods
Ren et al.	[132]	2022	Combined U-Net	UNet	Segmentation
Huang et al.	[134]	2022	Improved U-Net	UNet	Segmentation
Xu & Fan	[135]	2022	Dual semantic CNN	CNN	Segmentation
Zhong et al.	[136]	2022	MMDC-Net	UNet	Segmentation
Deng et al.	[138]	2022	Multiscale attention mechanism	Attention network	Segmentation
Huang et al.	[139]	2022	Cascaded self-attention	UNet	Segmentation
Pavani et al.	[140]	2022	Decoder/encoder network	UNet	Segmentation
Karlsson & Hardarson	[141]	2022	CNN based U-Net	UNet	Segmentation
Zhu et al.	[143]	2022	Inception U-Net	UNet	Segmentation
Yin et al.	[144]	2022	Multiple networks	UNet	Segmentation and classification
Renyuan Liu et al.	[146]	2023	dual attention Res2Unet	UNet	Segmentation
Meilin Liu et al.	[147]	2023	AA-WIGAN	UNet	Segmentation
Khan et al.	[145]	2023	Multiscale context Network	Reccurent Network	Segmentation

9) Specificity: This term denotes the ratio of negative cases that were accurately classified.

$$Specificity = \frac{Tn}{Tn + Fp} \tag{5}$$

10) Area under the curve (AUC): his metric characterizes the classifier's capability to distinguish between classes. A higher value of the Area Under the Curve (AUC) indicates superior performance.

$$AUC = \int_a^b F(x).dx \tag{6}$$

Table 6
Pros and cons of CNN used for Retinal vessel.

Advantages	Disadvantages	Accuracy range
Data management is executed with a high degree of proficiency, potentially leading to enhanced accuracy. The network's substantial depth equips it to manage intricate representations adeptly. It is skillfully constructed with residual blocks to mitigate the vanishing gradient issue. This design facilitates reduced gradients, bias, and improved data comprehension.	Increased parameter count can lead to information loss, consequently elongating network processing time. Inability to execute translational invariant procedures. Prone to generating deceptive results. Demands substantial computational resources.	0.79–0.97

Where a and b are the upper and lower limits on the curve, and F(x) is the equation of the curve.

11) Dice measure (DM): This measurement evaluates the degree of overlap between the predicted segmentations and the ground truth. Higher values indicate accurate predictions.

$$DM = 2 * \frac{/prediction \cap GT/}{/Prediction/ + /GT/} \tag{7}$$

12) F1 scores: measures the function of precision and recall.

$$F1 = 2 * \frac{Precision * Recall}{Precision + Recall} \tag{8}$$

13) Mathew correction coefficient (MCC): measures the number of true and false positives and negatives.

$$MCC = \frac{Tp * Tn - Fp * Fn}{\sqrt{(Tp + Fp)(Tp - Fn)(Tn + Fp)(Tn + Fn)}} \tag{9}$$

These metrics provide insights into the accuracy and effectiveness of the CNN methods in detecting and classifying abnormalities in retina fundus images.

5. Datasets

This section provides an overview of the datasets utilized for segmenting and classifying retina fundus images. The datasets are presented in the order of their usage, including DRIVE [160], STARE [161], CHASE-DB1 [162], HRF [163], MESSIDOR [164], IOSTAR [165], ORIGA [166], REFUGE [166], DB1 [167], DB0 [168], Kaggle dataset, DRISHTI-GS [169], NIVE [170], RIM-ONEr3 [171], DRIONS-DB [172], RITE [173], WIDE [174], SYNTHE [175], LES-AV [176], RIGA [177], DUKE, DCA, EIARG1, and AV-INSPIRE. Fig. 9 illustrates the list of datasets with the highest usage, while datasets with a usage count of less than 2 were excluded from the graph. The prominent datasets in terms of usage are DRIVE, STARE, CHASE-DB1, and HRF. It is evident that a valuable dataset should possess relevance, usability, and high-quality attributes [178]. Therefore, we posit that datasets with greater usage exemplify these aforementioned characteristics. In summary, the majority of databases discussed in this study are meticulously curated repositories of retinal fundus images. These databases represent invaluable assets for medical research, fostering the creation of sophisticated diagnostic tools and therapies to enhance both ocular health and patient well-being.

6. Analyses

The authors conducted a comprehensive search across various online repositories to identify research papers focused on the classification and segmentation of retina fundus images using CNN. Initially, a total of 300 papers were gathered through this search process. Subsequently, these papers underwent a screening process, resulting in a selection of 170 relevant papers. The authors then specifically focused on papers related to arteries, vessels, and optic discs/cups, as illustrated in Fig. 10. From the narrowed scope, a total of 80 research papers were included in this review, specifically addressing the classification and segmentation of veins, optic discs, and blood vessels using CNN. Among these papers, 60 were obtained from ScienceDirect, 15 from Springer, and 5 from other sources. While the authors made efforts to include all relevant research articles within the scope of their study, it is possible that some

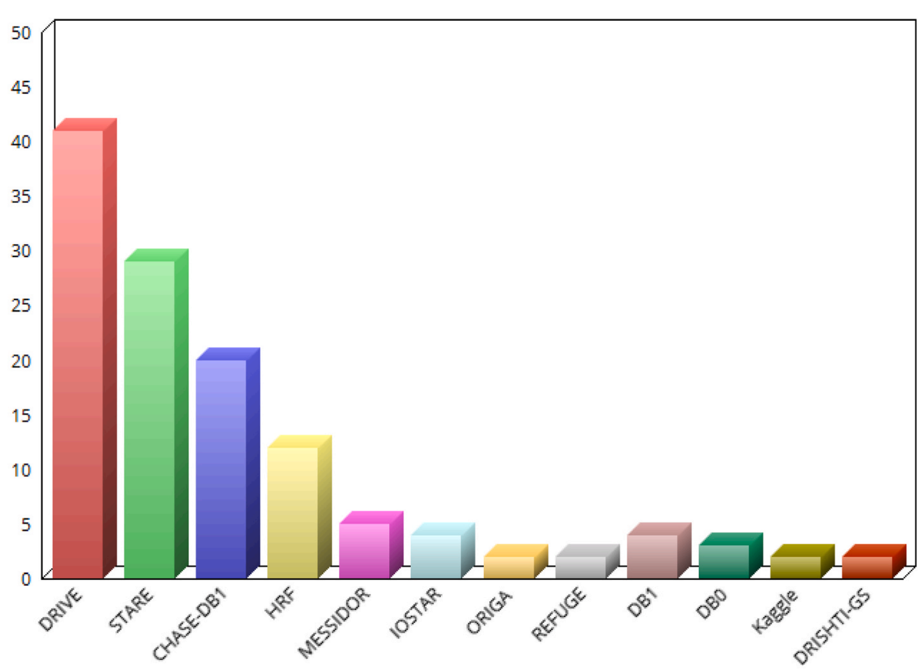

Fig. 9. Datasets used for classification and segmentation of retina fundus images.

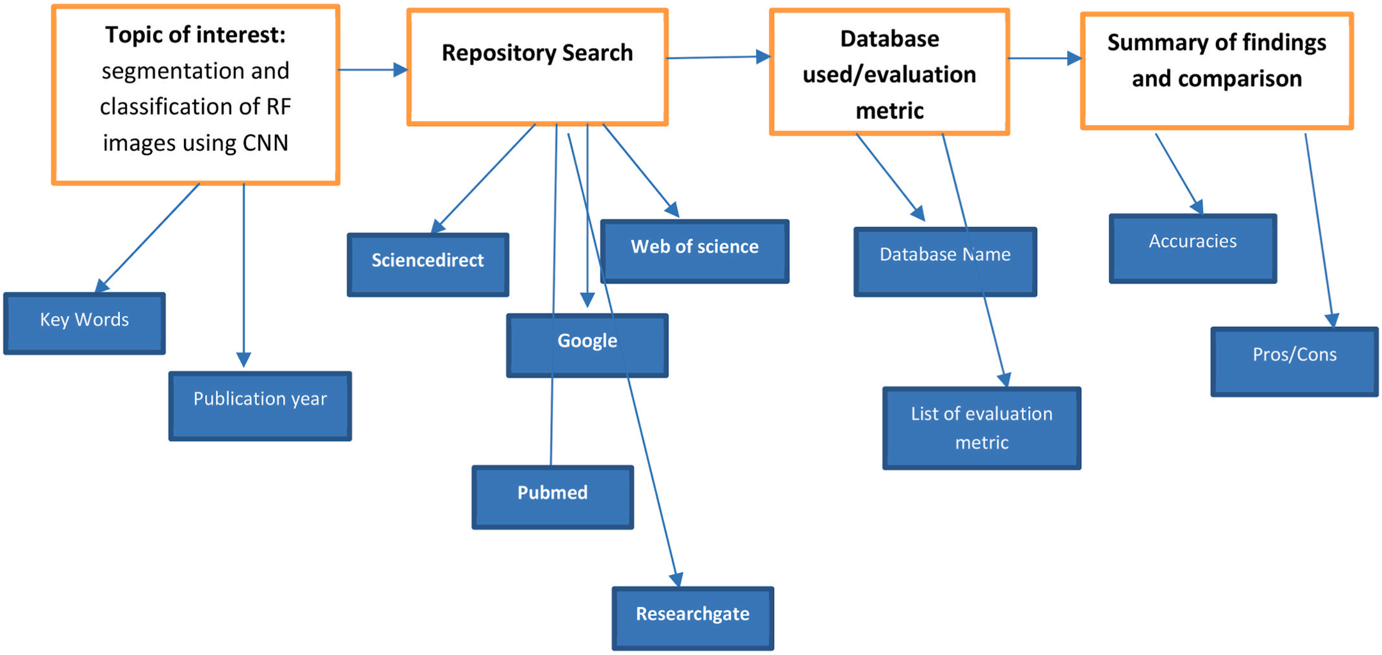

Fig. 10. Approach for the review process.

interesting studies may have been inadvertently overlooked.

For a more in-depth examination of the data origins and the dispersion of publications across various years, refer to Fig. 11. To explore the contrasts in accuracy between optic disc (OD) and optic cup (OC) segmentation, consult Fig. 12. Observing Fig. 12 reveals that the spectrum of achieved accuracies spans from a minimum of 86% to a maximum of 99%. Notably, a significant proportion of accuracy scores cluster within the range of 93%–96%. These visual representations serve to augment our understanding of the origins of the incorporated studies as well as the chronological distribution of research findings within the field.

This review encompassed a total of 2 papers focusing on arteries and veins, 15 papers on optic disc and cup, and 58 papers on retina vessels. Five additional research papers published in 2023 have utilized CNN for disease detection, employing the entire retinal fundus image for analysis. Among these, 4 studies employed a combination of CNN methods with traditional approaches, as indicated in Tables 6 and 2 Notably, reference [126] solely concentrated on classification, whereas references [127,128], and [100] presented segmentation and classification approaches specifically for retina fundus images. Fig. 12 provides an analysis of the accuracy metric specifically for the optic disc and cup. However, for a comprehensive overview of accuracy and other performance measures, referring to the tables is recommended, as they contain additional information on various metrics across different studies.

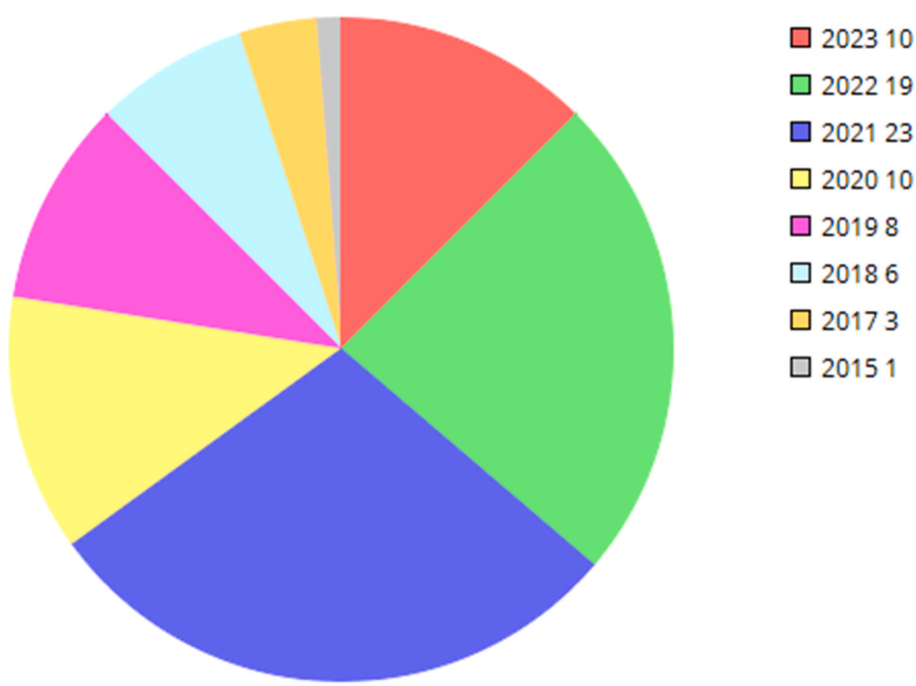

Fig. 11. Number of papers published yearly.

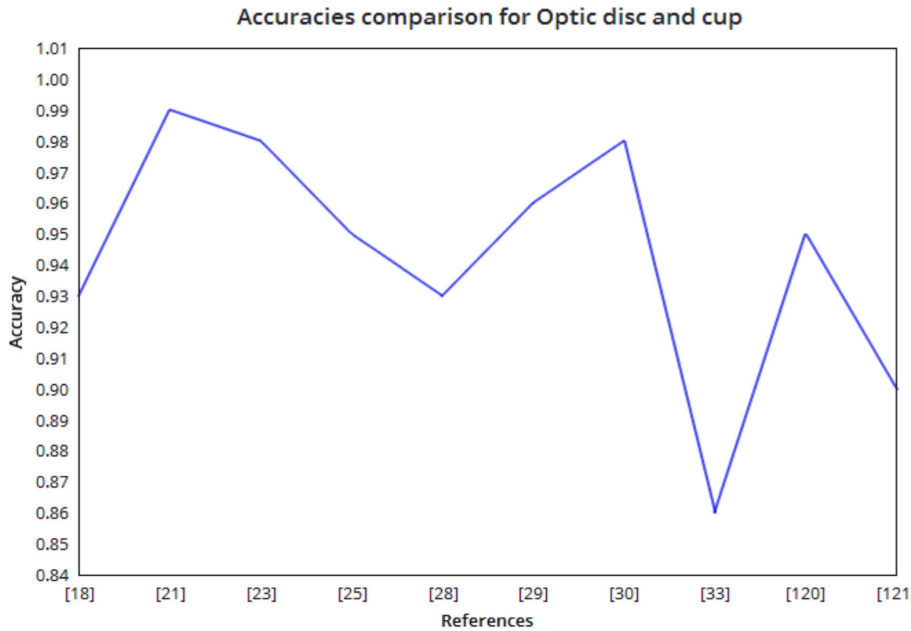

Fig. 12. Accuracy comparison for optic disc and cup.

7. Conclusions and future directions

The objective of this study is to provide a comprehensive review of CNN methods used for the segmentation and classification of retinal fundus images. These CNN algorithms have demonstrated impressive performance, achieving approximately 99% accuracy in certain cases. In the field of medical practice, these CNN methods have provided valuable insights that clinicians have utilized to draw conclusions about specific pathologies. They have aided in disease diagnosis and the prediction of ophthalmic conditions in patients. The overall performance of CNN algorithms in this domain has positioned them as promising alternatives to traditional methods. Notably, the IDX (Intact Dilated Extraction) technique has already gained approval for practical use in medium and large healthcare facilities, physician groups, and medical management firms [179,180,181]. As CNN algorithms continue to improve in stability and efficiency, their relevance is expected to be widely accepted, opening doors for their application in other critical areas of healthcare delivery.

7.1. Observations

- From the reviewed papers, it is evident that the majority of CNN methods for retinal fundus image segmentation are built upon the UNet, attention mechanisms, and adversarial networks. This preference can be attributed to the strong performance of these networks, particularly the UNet, in medical image tasks. Considering that retinal fundus image segmentation requires a network that accurately addresses the task, leveraging the UNet architecture is a suitable choice.
- The utilization of preprocessing methods has contributed to improved accuracy. Many researchers have employed techniques such as Contrast Limited Adaptive Histogram Equalization (CLAHE) for image enhancement and various filters for denoising. While the use of different denoising methods has not significantly enhanced results, the application of CLAHE for image enhancement has demonstrated performance improvements.
- Conversion of color retinal fundus images from RGB format to LAB and subsequent conversion back to RGB after preprocessing has been a common practice. This conversion facilitates a conducive environment for preprocessing procedures.
- Acquiring a large dataset is a challenge in medical image analysis due to limited availability. To address this, most CNN methods have employed data augmentation techniques as a preprocessing step to expand the dataset.
- Multilevel, multiscale, and multidirectional networks have been prevalent in papers published in 2022. These networks involve the combination of multiple encoder and decoder frameworks.
- Retinal vessel segmentation has emerged as the most commonly studied application of CNN methods for segmentation and classification, likely due to the prominent visibility of retinal vessels in fundus images.
- Recent trends involve incorporating attention mechanisms, Bilinear Feature Pyramid Networks (BIFPN), or other networks into the skip connections of the UNet architecture. Many CNN networks proposed in 2022 have adopted this approach.

7.2. Limitations and future directions

Although CNN algorithms have made significant contributions to fundus image segmentation and classification, there are still challenges that need to be addressed when applying CNN to retinal fundus (RF) images.

1) **Limited availability of labeled quality data**: The quality of the labeled data directly influences the performance of CNN algorithms, and obtaining a sufficient amount of accurately labeled data for RF images remains a challenge. One reason is that experts involved in labeling have busy schedules and may not have enough time to accomplish the task. For instance, achieving reliable labeling for breast ultrasound images typically requires the participation of three experts who perform the labeling and make majority-voting decisions to obtain the final labeled image. This process is demanding, time-consuming, and requires significant effort. To address this issue, researchers can explore methods like the ones described in Ref. [182], which involve a combination of algorithms and human supervision to generate labeled data. Additionally, weakly supervised methods can be employed to leverage the available labeled data and expand its usage in the context of unlabeled data. These approaches offer potential solutions to mitigate the scarcity of labeled data in RF image analysis. unlabeled data.

2) **Performance of CNN methods in a real-life situation**: Many of the CNN methods evaluated in this review lack testing in real-life scenarios, leaving uncertainty about their optimal performance when applied to practical applications. To address this concern, it is crucial for analysts and computer vision engineers to establish close collaboration with clinicians. By working hand-in-hand, these interdisciplinary teams can ensure a gradual and informed deployment of CNN algorithms in real-life settings. This collaborative approach allows for the integration of clinical expertise, validation studies, and iterative improvements, thereby enhancing the reliability and effectiveness of CNN algorithms when used in real-life applications.
3) **Unavailability of standard measuring metrics**: The use of diverse evaluation metrics for reporting quantitative results is evident in the research, as these metrics capture different aspects of performance. Consequently, authors have the flexibility to choose any metric from the available list to quantify their findings. While this review has addressed the issue to some extent by aggregating two common accuracies from the studies, there is still room for further efforts to minimize the proliferation of metrics. We propose the adoption of a standardized procedure that selects three or four metrics as a benchmark for the segmentation and classification of RF images. By establishing this standardized set of metrics, uniformity can be achieved in the evaluation process, allowing for better comparison and interpretation of results across different studies.
4) **CNN high computation space**: The resource-intensive nature of CNN algorithms is widely recognized, often necessitating a significant computational infrastructure. Inadequate computational resources can pose challenges to achieving higher accuracies in segmentation tasks. To address this issue, we call for the development of additional cloud computing platforms, such as Collab, that offer ample computational space. These platforms should be accessible to researchers at minimal or no cost, facilitating the execution of their applications and alleviating the burden of limited computational resources. By expanding the availability of such cloud computing platforms, researchers can harness the necessary computational power to enhance the performance of CNN algorithms in segmentation tasks without incurring substantial expenses.

Author contributions

All authors contributed to the study's conception and design. Material preparation and data collection were performed by AEI. Analysis was done by AEI, TI., AG. The manuscript was written and polished by AEI.

Funding

No funding applicable to this research.

Declaration of competing interest

The authors declare that they have no known competing financial interests or personal relationships that could have appeared to influence the work reported in this paper.

Data availability

No data was used for the research described in the article.

Acknowledgements

We would like to sincerely express our deep gratitude to our esteemed mentors: Professor David A. Wolk from the Penn Memory Center at the University of Pennsylvania, Professor Sandhitsu Das from PICSL at the University of Pennsylvania, Professor Jayaram K. Udupa and Professor Drew A. Torigian from the MIPG at the University of Pennsylvania, and Professor Stanislav Makhanov at SIIT Thammassat University. We also extend our heartfelt thanks to the management of Alex Ekwueme Federal University Nigeria, as well as the anonymous referees of the review, for their invaluable remarks and significant contributions.

References

[1] World Health Organization, Blindness and Vision Impairment, 2022. https://www.who.int/news-room/fact-sheets/detail/blindness-and-visual-impairment. June 19 2023.
[2] S. Sengupta, A. Singh, H.A. Leopold, T. Gulati, V. Lakshminarayanan, Ophthalmic diagnosis using deep learning with fundus images - a critical review, Artif. Intell. Med. 102 (2020 Jan), 101758, https://doi.org/10.1016/j.artmed.2019.101758. Epub 2019 Nov 22. PMID: 31980096.
[3] M.T. Nicolela, J.R. Vianna, Pearls of Glaucoma Management, in: Optic Nerve: Clinical Examination, Springer, Berlin, Heidelberg, 2016, pp. 17–26.
[4] T. Aziz, A.E. Ilesanmi, C. Charoenlarpnopparut, Efficient and accurate hemorrhages detection in retinal fundus images using smart window features, Appl. Sci. 11 (2021) 6391, https://doi.org/10.3390/app11146391.
[5] A.S. Krolewski, J.H. Warram, L.I. Rand, A.R. Christlieb, E.J. Busick, C.R. Kahn, Risk of proliferative diabetic retinopathy in juvenile-onset type I diabetes: a 40-yr follow-up study, Diabetes Care 9 (5) (1986) 443–452.
[6] T. Kauppi, V. Kalesnykiene, J.K. Kamarainen, L. Lensu, I. Sorri, H. Uusitalo, H. Kälviäinen, J. Pietilä, DIARETDB0: evaluation database and methodology for diabetic retinopathy algorithms, Machine Vision and Pattern Recognition Research Group, Lappeenranta University of Technology: Lappeenranta, Finland 73 (2006) 1–17.
[7] Age-Related Eye Disease Study Research Group, The relationship of dietary carotenoid with vitamin A, E, and C intake with age-related macular degeneration in a case-control study, Arch. Ophthalmol. 125 (9) (2007) 1225–1232.
[8] Age-Related Eye Disease Study Research Group, Risk factors associated with age-related nuclear and cortical cataracts, Ophthalmol. Times 108 (8) (2001) 1400–1408.
[9] U.S. Department, Of Health and Human Services, Office of the Surgeon General, The Health Consequences of Smoking: A Report of the Surgeon General, Washington, D.C, 2004.
[10] M.J. Fowler, Microvascular and macrovascular complications of diabetes, Clin. Diabetes 26 (2) (2008) 77–82.
[11] ETDRSR. Group, Grading diabetic retinopathy from stereoscopic color fundus photographs—an extension of the modified Airlie House classi- fication: ETDRS report number 10, Ophthalmol. Times 98 (5) (1991) 786–806.
[12] C.J. Rudnisky, B.J. Hinz, M.T. Tennant, A.R. de Leon, M.D. Greve, High-resolution stereoscopic digital fundus photography versus contact lens biomicroscopy for the detection of clinically significant macular edema, Ophthalmol. Times 109 (2) (2002) 267–274.
[13] Md Mohaimenul Islam, Hsuan-Chia Yang, Tahmina Nasrin Poly, Wen-Shan Jian, Yu-Chuan (Jack) Li, Deep learning algorithms for detection of diabetic retinopathy in retinal fundus photographs: a systematic review and meta-analysis, Comput. Methods Progr. Biomed. 191 (2020), 105320.
[14] C. L Srinidhi, P. Aparna, J. Rajan, Recent advancements in retinal vessel segmentation, J. Med. Syst. 41 (2017) 70, https://doi.org/10.1007/s10916-017-0719-2.
[15] https://www.invision2020.com/retinal-imaging-history/. (Accessed 10 October 2021).
[16] Ademola Enitan Ilesanmi, Oluwagbenga Paul Idowu, Stanislav S. Makhanov, Multiscale superpixel method for segmentation of breast ultrasound, Comput. Biol. Med. 125 (2020), 103879.
[17] Yang Chen, Guirong Weng, An active contour model based on local pre-piecewise fitting image, Optik (2021), 168130.
[18] Daniel Lacker, Kavita Ramanan, Ruoyu Wu, Locally interacting diffusions as Markov random fields on path space,Stochastic Processes and their Applications 140 (2021) 81–114.
[19] O. Ronneberger, P. Fischer, T. Brox, U-net: convolutional networks for biomedical image segmentation, in: Conference on Medical Image Computing and Computer Assisted Intervention (MICCAI), 2015.
[20] N. Siddique, S. Paheding, C.P. Elkin, V. Devabhaktuni, U-net and its variants for medical image segmentation: a review of theory and applications, IEEE Access 9 (2021) 82031–82057, https://doi.org/10.1109/ACCESS.2021.3086020.
[21] Rohit Thanki, A deep neural network and machine learning approach for retinal fundus image classification, Healthcare Analytics 3 (2023), 100140.
[22] M.S.B. Phridviraj, Raghuram Bhukya, Sujatha Madugula, Aakunuri Manjula, Swathy Vodithala, Mohammed Sharfuddin Waseem, A bi-directional Long Short-Term Memory-based Diabetic Retinopathy detection model using retinal fundus images, Healthcare Analytics 3 (2023), 100174.
[23] Kamesh Sonti, Ravindra Dhul, A new convolution neural network model "KR-NET'' for retinal fundus glaucoma classification, Optik 283 (2023), 170861.
[24] V.M. Raja Sankari, U. Snekhalatha, Ashok Chandrasekaran, Prabhu Baskaran, Automated diagnosis of Retinopathy of prematurity from retinal images of preterm infants using hybrid deep learning techniques, Biomed. Signal Process Control 85 (2023), 104883.

[25] L. Yanhong, S. Ji, Y. Lei, B. Guibin, Y. Hongnian, ResDO-Unet, A deep residual network for accurate retinal vessel segmentation from fundus images, Biomed. Signal Process Control 79 (1) (2023), https://doi.org/10.1016/j.
[26] Lei Wang, Juan Gu, Yize Chen, Yuanbo Liang, Weijie Zhang, Jiantao Pu, Hao Chen, Automated segmentation of the opt ic disc from fundus images using an asymmetric deep learning network, Pattern Recogn. 112 (2021), 107810.
[27] Yinghua Fu, Jie Chen, Li Jiang, Dongyan Pan, Xuezheng Yue, Yiming Zhu, Optic disc segmentation by U-net and probability bubble in abnormal fundus images, Pattern Recogn. 117 (2021), 107971.
[28] H. Narasimhaiyer, A. Can, B. Roysam, V. Stewart, H.L. Tanenbaum, A. Majerovics, H. Singh, Robust detection and classification of longitudinal changes in color retinal fundus images for monitoring diabetic retinopathy, IEEE Trans. Biomed. Eng. 53 (6) (2006) 1084–1098.
[29] Xianjing Meng, Xiaoming Xi, Yang Lu, Guang Zhang, Yilong Yin, Xinjian Chen, Fast and effective optic disk localization based on convolutional neural network, Neurocomputing 312 (2018) 285–295.
[30] Xin Yuan, Lingxiao Zhou, Shuyang Yu, Miao Li, Xiang Wang, Xiujuan Zheng, A multi-scale convolutional neural network with context for joint segmentation of optic disc and cup, Artif. Intell. Med. 113 (2021), 102035.
[31] Ademola Enitan Ilesanmi, Utairat Chaumrattanakul, Stanislav S. Makhanov, A method for segmentation of tumors in breast ultrasound images using the variant enhanced deep learning, Biocybern. Biomed. Eng. 41 (2) (2021) 802–818.
[32] H. Fu, J. Cheng, Y. Xu, D.W.K. Wong, J. Liu, X. Cao, Joint optic disc and cup segmentation based on multi-label deep network and polar transformation, IEEE Trans. Med. Imag. 37 (7) (2018) 1597–1605.
[33] Lei Wang, Liu Han, Yaling Lu, Hang Chen, Jian Zhang, Jiantao Pu, A coarse-to-fine deep learning framework for optic disc segmentation in fundus images, Biomed. Signal Process Control 51 (2019) 82–89.
[34] Jen Hong Tan, U. Rajendra Acharya, Sulatha V. Bhandary, Chua Chua Kuang, Segmentation of optic disc, fovea and retinal vasculature using a single convolutional neural network, Journal of Computational Science 20 (2017) 70–79.
[35] H.N. Veena, A. Muruganandham, T. Senthil Kumaran, A novel optic disc and optic cup segmentation technique to diagnose glaucoma using deep learning convolutional neural network over retinal fundus images, Journal of King Saud University – Computer and Information Sciences 34 (2022) 6187–6198.
[36] Neha Mathur, Shruti Mathur, Divya Mathur, A novel approach to improve Sobel edge detector, Proc. Comput. Sci. 93 (2016) 431–438.
[37] Lei Zhang, Lang Zou, Chuanyu Wu, Jiangming Jia, Jianneng Chen, Method of famous tea sprout identification and segmentation based on improved watershed algorithm, Comput. Electron. Agric. 184 (2021), 106108.
[38] Rakhshanda Imtiaz, M. Tariq, Khan, Syed saud naqvi, muhammad arsalan, syed junaid nawaz, screening of glaucoma disease from retinal vessel images using semantic segmentation, Comput. Electr. Eng. 91 (2021), 107036.
[39] Zhe Xie, Tonghui Ling, Yuanyuan Yang, Rong Shu, Brent J. Liu, Optic disc and cup image segmentation utilizing contour-based transformation and sequence labeling networks, J. Med. Syst. 44 (2020) 96.
[40] B. Xu, N. Wang, T. Chen, M. Li, Empirical Evaluation of Rectified Activations in Convolutional Network, 2015, pp. 1–5, arXiv: 1505.00853vol. 2.
[41] A. Viterbi, Optimum detection and signal selection for partially coherent binary communication, IEEE Trans. Inf. Theor. 11 (2) (Apr. 1965) 239–246.
[42] A.J. Viterbi, A personal history of the Viterbi algorithm, IEEE Signal Process. Mag. 23 (4) (Jul. 2006) 120–142.
[43] Sandip Sadhukhan, Arpita Sarkar, Debprasad Sinha, Goutam Kumar Ghorai, Gautam Sarkar, Ashis K. Dhara, Attention based fully convolutional neural network for simultaneous detection and segmentation of optic disc in retinal fundus images, World academy of science, Engineering and Technology International Journal of Medical and Health Sciences 14 (8) (2020).
[44] R. Priyanka, S.J. Grace Shoba, A. Brintha Therese, Segmentation of optic disc in fundus images using convolutional neural networks for detection of glaucoma, International Journal of Advanced Engineering Research and Science (IJAERS) 4 (Issue 5) (2017).
[45] F. Hoppner, F. Klawonn, A contribution to convergence theory of fuzzy c-means and derivatives, IEEE Trans. Fuzzy Syst. 11 (5) (2003) 682–694.
[46] C. Raja, N. Vinodhkumar, An efficient segmentation of optic disc using convolution neural network for glaucoma detection in retinal images, European Journal of Molecular & Clinical Medicine 7 (Issue 03) (2020).
[47] A.Z.M.E. Chowdhury, G. Mann, W.H. Morganb, A. Vukmirovic, A. Mehnert, F. Sohel, Msganet-Rav, A multiscale guided attention network for artery-vein segmentation and classification from the optic disc and retinal images, Journal of Optometry 15 (2022) S58S69, https://doi.org/10.1016/j.optom.2022.11.001.
[48] Á.S. Hervella *, J. Rouco, J. Novo, M. Ortega, End-to-end multi-task learning for simultaneous optic disc and cup segmentation and glaucoma classification in eye fundus images, Appl. Soft Comput. 116 (2022), 108347.
[49] Indresh Kumar Gupta, Abha Choubey, Siddhartha Choubey, Mayfly optimization with deep learning enabled retinal fundus image classification model, Comput. Electr. Eng. 102 (2022), 108176.
[50] K. Zervoudakis, S. Tsafarakis, A mayfly optimization algorithm, Comput. Ind. Eng. 145 (2020), 106559.
[51] H.N. Veena, A. Muruganandham, T. Senthil Kumaran, A novel optic disc and optic cup segmentation technique to diagnose glaucoma using deep learning convolutional neural network over retinal fundus images, Journal of King Saud University – Computer and Information Sciences 34 (2022) 6187–6619.
[52] Hao Xiong, Sidong Liu, Roneel V. Sharan, Enrico Coiera, Shlomo Berkovsky, Weak label based Bayesian U-Net for optic disc segmentation in fundus images, Artif. Intell. Med. 126 (2022), 102261.
[53] Souvik Maiti, Debasis Maji, Ashis Kumar Dhara, Gautam Sarkar, Automatic detection and segmentation of optic disc using a modified convolution network, Biomed. Signal Process Control 76 (2022), 103633.
[54] Rajarshi Bhattacharya, Rukhshanda Hussain, Agniv Chatterjee, Dwipayan Paul, Saptarshi Chatterjee, Debangshu Dey, Py-Net, Rethinking segmentation frameworks with dense pyramidal operations for optic disc and cup segmentation from retinal fundus images, Biomed. Signal Process Control 85 (2023), 104895.
[55] A. Septiarini, H. Hamdani, E. Setyaningsih, E. Junirianto, F. Utaminingrum, Automatic method for optic disc segmentation using deep learning on retinal fundus images, Healthc Inform Res 29 (2) (2023 Apr) 145–151, https://doi.org/10.4258/hir.2023.29.2.145. Epub 2023 Apr 30. PMID: 37190738; PMCID: PMC10209731.
[56] H. Fu, J. Cheng, Y. Xu, D. Wong, J. Liu, X. Cao, Joint optic disc and cup segmentation based on multi-label deep network and polar transformation, IEEE Trans. Med. Imag. 37 (7) (2018) 1597–1605.
[57] Y. LeCun, L. Bottou, Y. Bengio, P. Haffner, Gradient-based learning applied to document recognition, Proc. IEEE 86 (11) (1998) 2278–2324.
[58] F. Yu, V. Koltun, Multi-scale context aggregation by dilated convolutions, in: 4th International Conference on Learning Representations, ICLR 2016 - Conference Track Proceedings, 2016.
[59] Fantin Girarda, Conrad Kavalec, Farida Cheriet, Joint segmentation and classification of retinal arteries/veins from fundus images, Artif. Intell. Med. 94 (2019) 96–109.
[60] Jos′e Morano, ′Alvaro S. Hervella, Jorge Novo, Jos′e Rouco, Simultaneous segmentation and classification of the retinal arteries and veins from color fundus images, Artif. Intell. Med. 118 (2021), 102116.
[61] C. Wang, Z. Zhao, Y. Yu, Fine retinal vessel segmentation by combining Nest U-net and patch-learning, Soft Comput. 25 (2021) 5519–5532, https://doi.org/10.1007/s00500-020-05552-w.
[62] M. Kaur, A. Kamra, Detection of retinal abnormalities in fundus image using transfer learning networks, Soft Comput. (2021), https://doi.org/10.1007/s00500-021-06088-3.
[63] F. Girard, C. Kavalec, F. Cheriet, Joint segmentation and classification of retinal arteries/veins from fundus images, Artif. Intell. Med. 94 (2019) 96–109, https://doi.org/10.1016/j.artmed.2019.02.004.
[64] Ümit Budak, Zafer Cömert, Musa Çıbuk, Abdulkadir Şengür, Dccmed-Net, Densely connected and concatenated multi Encoder-Decoder CNNs for retinal vessel extraction from fundus images, Med. Hypotheses 134 (2020), 109426.
[65] Tanga Peng, Qiaokang Lianga, Xintong Yana, Dan Zhang, Gianmarc Coppola, Wei Sun, Multi-proportion channel ensemble model for retinal vessel segmentation, Comput. Biol. Med. 111 (2019), 103352.
[66] J. Odstrcilik, et al., Retinal vessel segmentation by improved matched filtering: evaluation on a new high-resolution fundus image database, IET Image Process. 7 (4) (2013) 373–383.
[67] Zhao He, Yun Sun, Huiqi Li, Retinal vascular junction detection and classification via deep neural networks, Comput. Methods Progr. Biomed. 183 (2020), 105096.
[68] K. He, X. Zhang, S. Ren, J. Sun, Deep residual learning for image recognition, in: Proceedings of the IEEE Conference on Computer Vision and Pattern Recognition, 2016, pp. 770–778.
[69] Ruohan Zhao, Li Qin, Jianrong Wu, Jane You, A nested U-shape network with multi-scale upsample attention for robust retinal vascular segmentation, Pattern Recogn. 120 (2021), 107998.
[70] T.-Y. Lin, P. Dollar, R. Girshick, K. He, B. Hariharan, S. Belongie, Feature pyramid networks for object detection, in: Proceedings of the IEEE Conference on Computer Vision and Pattern Recognition, 2017, pp. 2117–2125.
[71] Maciej Czepita, Anna Fabija ́nska, Image processing pipeline for the detection of blood flow through retinal vessels with subpixel accuracy in fundus images, Comput. Methods Progr. Biomed. 208 (2021), 106240.
[72] S. Klein, Staring, M.K. Murphy, M.A. Viergever, J.P.W. Pluim, Elastix: a toolbox for intensity based medical image registration, IEEE Trans. Med. Imag. 29 (1) (2010) 196–205, https://doi.org/10.1109/TMI.2009.2035616.
[73] L.D. Hubbard, R.J. Brothers, W.N. King, et al., Methods for evaluation of retinal microvascular abnormalities associated with hypertension/sclerosis in the atherosclerosis risk in communities study, Ophthalmol. Times 106 (12) (1999) 2269–2280 Dec, https://doi.org/10.1016/s0161-6420(99)90525-0.
[74] Gang Sun, Xiaoyan Liu, Xuefei Yu, Multi-path cascaded U-net for vessel segmentation from fundus fluorescein angiography sequential images, Comput. Methods Progr. Biomed. 211 (2021), 106422.
[75] Michael Yeung, Evis Sala, Carola-Bibiane Schonlieb, Leonardo Rundo, Focus U-Net, A novel dual attention-gated CNN for polyp segmentation during colonoscopy, Comput. Biol. Med. 137 (2021), 104815.
[76] Lei Sang, Min Xu, Shengsheng Qian, Xindong Wu, Knowledge graph enhanced neural collaborative filtering with residual recurrent network, Neurocomputing 454 (2021) 417–429.
[77] J.V. Soares, J.J. Leandro, R.M. Cesar, H.F. Jelinek, M.J. Cree, Retinal vessel segmentation using the 2-D Gabor wavelet and supervised classification, IEEE Trans. Med. Imag. 25 (9) (2006) 1214–1222.
[78] Song Guo, Kai Wang, Hong Kang, Yujun Zhang, Yingqi Gao, Tao Li, Bts-Dsn, Deeply supervised neural network with short connections for retinal vessel segmentation, Int. J. Med. Inf. 126 (2019) 105–113.
[79] Yanhui Guo, Ümit Budak, Abdulkadir ̧S engür, A novel retinal vessel detection approach based on multiple deep convolution neural networks, Comput. Methods Progr. Biomed. 167 (2018) 43–48.
[80] Zhongshuo Zhuo, Jianping Huang, Ke Lu, Daru Pan, A size-invariant convolutional network with dense connectivity applied to retinal vessel

segmentation measured by a unique index, Comput. Methods Progr. Biomed. 196 (2020), 105508.
[81] Y. Luo, H. Cheng, L. Yang, Size-invariant fully convolutional neural network for vessel segmentation of digital retinal images, in: Signal and Information Processing Association Annual Summit and Conference (APSIPA), 2016 Asia-Pacific, IEEE, 2016, pp. 1–7.
[82] G. Huang, Z. Liu, L. Van Der Maaten, K.Q. Weinberger, Densely connected convolutional networks, CVPR 1 (2017) 3.
[83] Álvaro S. Hervella, Jorge Novo JoséRouco, ManuelG. Penedo, Marcos Ortega, Deep multi-instance heatmap regression for the detection of retinal vessel crossings and bifurcations in eye fundus images, Comput. Methods Progr. Biomed. 186 (2020), 105201.
[84] S. Pearl Mary, V. Thanikaiselvan, Unified adaptive framework for contrast enhancement of blood vessels, Int. J. Electr. Comput. Eng. 10 (2020) 767–777, https://doi.org/10.11591/ijece.v10i1.pp767-777.
[85] K. Simonyan, A. Zisserman, Very deep convolutional networks for large-scale image recognition, in: 3rd Int. Conf. Learn. Represent. ICLR 2015 - Conf, Track Proc., 2015.
[86] Di Li, Susanto Rahardja, BseresU-Net, An attention-based before-activation residual U-Net for retinal vessel segmentation, Comput. Methods Progr. Biomed. 205 (2021), 106070.
[87] Zefang Lin, Jianping Huang, Yingyin Chen, Xiao Zhang, Wei Zhao, Yong Li, Ligong Lu, Meixiao Zhan, Xiaofei Jiang, Xiong Liang, A high resolution representation network with multi-path scale for retinal vessel segmentation, Comput. Methods Progr. Biomed. 208 (2021), 106206.
[88] C. Meng, K. Sun, S. Guan, Q. Wang, R. Zong, L. Liu, Multiscale dense convolutional neural network for DSA cerebrovascular segmentation, Neurocomputing 373 (2020) 123–134.
[89] Chun Tian, Tao Fang, Yingle Fan, Wei Wu, Multi-path convolutional neural network in fundus segmentation of blood vessels, biocybernetic and biomedical engineering 40 (2020) 583–595.
[90] Ibrahim Atli, Osman Serdar Gedik, Sine-Net: a fully convolutional deep learning architecture for retinal blood vessel segmentation, Engineering Science and Technology, Int. J. 24 (2021) 271–283.
[91] X. Bai, F. Zhou, B. Xue, Image enhancement using multi-scale image features extracted by top-hat transform, Opt Laser. Technol. 44 (2) (2012) 328–336.
[92] Yanhui Guo, Ümit Budak, J. Lucas, Vespa, Elham Khorasani, Abdulkadir Şengür, A retinal vessel detection approach using convolution neural network with reinforcement sample learning strategy, Measurement 125 (2018) 586–591.
[93] L.C. Chen, G. Papandreou, I. Kokkinos, K. Murphy, A.L. Yuille, Deeplab: semantic image segmentation with deep convolutional nets, atrous convolution, and fully connected crfs, IEEE Trans. Pattern Anal. Mach. Intell. 40 (4) (2018) 834–848, https://doi.org/10.1109/tpami.2017.2699184.
[94] Yicheng Wu, Yong Xia, Yang Song, Yanning Zhang, Weidong Cai, NFN+: a novel network followed network for retinal vessel segmentation, Neural Network. 126 (2020) 153–162.
[95] Ruben Hemelings, Bart Elend, Ingeborg Stalmans, Karel Van Keer, Patrick De Boever, Matthew B. Blaschko, Artery–vein segmentation in fundus images using a fully convolutional network, Comput. Med. Imag. Graph. 76 (2019), 101636.
[96] J.V.B. Soares, J.J.G. Leandro, R.M. Cesar, H.F. Jelinek, M.J. Cree, Retinal vessel segmentation using the 2-d gabor wavelet and supervised classification, IEEETrans. Med. Imaging 25 (2006) 1214–1222.
[97] Henda Boudegga, Yaroub Elloumi, Mohamed Akil, Mohamed Hedi Bedoui, Rostom Kachouri, Asma Ben Abdallah, Fast and efficient retinal blood vessel segmentation method based on deep learning network, Comput. Med. Imag. Graph. 90 (2021), 101902.
[98] Z. Jiang, H. Zhang, Y. Wang, S.-B. Ko, Retinal blood vessel segmentation using fully convolutional network with transfer learning, Comput. Med. Imag. Graph. 68 (September) (2018) 1–15, https://doi.org/10.1016/j.compmedimag.2018.04.005.
[99] P. Liskowski, K. Krawiec, Segmenting retinal blood vessels with deep neural networks, IEEE Trans. Med. Imag. 35 (11) (2016) 2369–2380, https://doi.org/10.1109/TMI.2016.2546227. November.
[100] Shuangling Wang, Yilong Yin, Guibao Cao, Benzheng Wei, Yuanjie Zheng, Hierarchical retinal blood vessel segmentation based on feature and ensemble learning, Neurocomputing 149 (2015) 708–717.
[101] L. Breiman, Random forests, Mach. Learn. 45 (2001) 5–32.
[102] Kai Hu, Zhenzhen Zhang, Xiaorui Niu, Yuan Zhang, Chunhong Cao, Fen Xiao, Xieping Gao, Retinal vessel segmentation of color fundus images using multiscale convolutional neural network with an improved cross-entropy loss function, Neurocomputing 309 (2018) 179–191.
[103] Yukun Zhou, Zailiang Chen, Hailan Shen, Xianxian Zheng, Rongchang Zhao, Xuanchu Duan, A refined equilibrium generative adversarial network for retinal vessel segmentation, Neurocomputing 437 (2021) 118–130.
[104] A. Vaswani, N. Shazeer, N. Parmar, J. Uszkoreit, L. Jones, A.N. Gomez, et al., Attention is all you need, in: International Conference on Learning Representations, Long Beach, California, USA, 2017.
[105] Lei Yang, Huaixin Wang, Qingshan Zeng, Yanhong Liu, Guibin Bian, A hybrid deep segmentation network for fundus vessels via deep-learning framework, Neurocomputing 448 (2021) 168–178.
[106] Qiangguo Jin, Zhaopeng Meng, Tuan D. Pham, Qi Chen, Leyi Wei, Ran Su, Dunet, A deformable network for retinal vessel segmentation, Knowl. Base Syst. 178 (2019) 149–162.
[107] Toufique Ahmed Soomro, Ahmed J. Afifib, Junbin Gao, Olaf Hellwich, Lihong Zheng, Manoranjan Paul, Strided fully convolutional neural network for boosting the sensitivity of retinal blood vessels segmentation, Expert Syst. Appl. 134 (2019) 36–52.
[108] T.A. Soomro, A.J. Afifi, J. Gao, O. Hellwich, M.U. Khan, M. Paul, L. Zheng, Boosting sensitivity of a retinal vessel segmentation algorithm with convolutional neural network, in: International Conference on Digital Image Computing: Techniques and Applications (DICTA), 2017.
[109] Chala Mohamed, Benayad Nsiri, My Hachem El yousfi Alaoui, Abdelmajid Soulaymani, Abdelrhani Mokhtari, Brahim Benaji Chandler, An automatic retinal vessel segmentation approach based on Convolutional Neural Networks, Expert Syst. Appl. 184 (2021), 115459.
[110] Muyi Sun, Kaiqi Li, Xingqun Qi, Hao Dang, Guanhong Zhang, Contextual information enhanced convolutional neural networks for retinal vessel segmentation in color fundus images, J. Vis. Commun. Image Represent. 77 (2021), 103134.
[111] Huisi Wu, Wei Wang, Jiafu Zhong, Baiying Lei, Zhenkun Wen, Jing Qin, Scs-Net, A scale and context sensitive network for retinal vessel segmentation, Med. Image Anal. 70 (2021), 102025.
[112] V. Sathananthavathi, G. Indumathi, Encoder enhanced atrous (EEA) unet architecture for retinal blood vessel segmentation, Cognit. Syst. Res. 67 (2021) 84–95.
[113] Y. Fisher, V. Koltun, Multi-scale context aggregation by dilated convolutions, in: Proceeding of Computer Vision and Pattern Recognition ICLR 2016, 2016 arXiv:1511.07122v3 [cs.CV] 30 Apr 2016.
[114] Pengshuai Yin, Hongmin Cai, Qingyao Wu, Df-Net, Deep fusion network for multi-source vessel segmentation, Inf. Fusion 78 (2022) 199–208.
[115] H. Zhao, J. Shi, X. Qi, X. Wang, J. Jia, Pyramid scene parsing network, in: Proceedings of the IEEE Conference on Computer Vision and Pattern Recognition, 2017, pp. 2881–2890.
[116] Xianlun Tang, Bing Zhong, Jiangping Peng, Bohui Hao, Jie Li, Multi-scale channel importance sorting and spatial attention mechanism for retinal vessels segmentation, Applied Soft Computing Journal 93 (2020), 106353.
[117] Aamer Abdul Rahman, Birendra Biswal, P. Geetha Pavani, Shazia Hasan, M.V. S. Sairam, Robust segmentation of vascular network using deeply cascaded AReN-UNet, Biomed. Signal Process Control 69 (2021), 102953.
[118] R. Collobert, S. Bengio, Links between perceptrons, MLPs and SVMs, Proc. Int'l Conf. on Machine Learning (ICML) (2004).
[119] Zhengjin Shi, Tianyu Wang, Zheng Huang, Feng Xie, Zihong Liu, Bolun Wang, Jing Xu, Md-Net, A multi-scale dense network for retinal vessel segmentation, Biomed. Signal Process Control 70 (2021), 102977.
[120] Beaudelaire Saha Tchinda, Daniel Tchiotsop, Michel Noubom, Valerie Louis-Dorr, Didier Wolf, Retinal blood vessels segmentation using classical edge detection filters and the neural network, Inform. Med. Unlocked 23 (2021), 100521.
[121] J.V. Soares, J.J. Leandro, R.M. Cesar, H.F. Jelinek, M.J. Cree, Retinal vessel segmentation using the 2-d gabor wavelet and supervised classification, IEEE Trans. Med. Imag. 25 (9) (2006) 1214–1222.
[122] D. Ziou, S. Tabbone, Edge detection techniques- an overview, International Journal of Pattern Recognition and Image Analysis 8 (4) (1998) 537–559.
[123] J. Canny, A computational approach to edge detection, IEEE Trans. Pattern Anal. Mach. Intell. 8 (1986) 679–714.
[124] R.C. Gonzalez, R.E. Woods, S.L. Eddins, Digital Image Processing Using MATLAB, Pearson/Prentice Hall, Upper Saddle River, New Jersey, 2004.
[125] Manuel E. Gegundez-Arias, Diego Marin-Santos, Manuel J. Isaac Perez-Borrero, Vasallo-Vazquez, new deep learning method for blood vessel segmentation in retinal images based on convolutional kernels and modified U-Net model, Comput. Methods Progr. Biomed. 205 (2021), 106081.
[126] Debasis Maji, Arif Ahmed Sekh, Automatic grading of retinal blood vessel in deep retinal image diagnosis, J. Med. Syst. 44 (2020) 180.
[127] S.N. Sangeethaa, P. Uma Maheswari, An intelligent model for blood vessel segmentation in diagnosing DR using CNN, J. Med. Syst. 42 (2018) 175.
[128] Revathi Priya Muthusamy, S. Vinod, M. Tholkapiyan, Automatic detection of abnormalities in retinal blood vessels using DTCWT, GLCM feature extractor and CNN-rnn classifier, Int. J. Recent Technol. Eng. 8 (Issue 1S4) (2019).
[129] Retinal vessel segmentation via A coarse-to-fine convolutional neural network, in: IEEE International Conference on Bioinformatics and Biomedicine (BIBM), 2018.
[130] C. Shi, C. Xu, J. He, Y. Chen, Y. Cheng, Q. Yang, H. Qiu, Graph-based convolution feature aggregation for retinal vessel segmentation, Simulat. Model. Pract. Theor. 121 (2022), 102653.
[131] Song Guo, Csgnet, Cascade semantic guided net for retinal vessel segmentation, Biomed. Signal Process Control 78 (2022), 103930.
[132] Kan Ren, Longdan Chang, Minjie Wan, Guohua Gu, Qian Chen, An improved U-net based retinal vessel image segmentation method, Heliyon 8 (2022), e11187.
[133] M. Tan, R. Pang, Q.V. Le, EfficientDet: Scalable and Efficient Object Detection, IEEE/CVF Conference on Computer Vision and Pattern Recognition (CVPR), 2020, pp. 10778–10787.
[134] J. Han, Y. Wang, H. Gong, Fundus Retinal Vessels Image Segmentation Method Based on Improved U-Net, https://doi.org/10.1016/j.irbm.2022.03.001.
[135] Yanan Xu, Yingle Fan, Dual-channel asymmetric convolutional neural network for an efficient retinal blood vessel segmentation in eye fundus images, Biocybern. Biomed. Eng. 42 (2022) 695–706.
[136] Zhong Xiang, Hongbin Zhang, Guangli Li, Donghong Ji, Do you need sharpened details? Asking MMDC-Net: multi-layer multi-scale dilated convolution network for retinal vessel segmentation, Comput. Biol. Med. 150 (2022), 106198.
[137] Dora E. Alvarado-Carrillo, Oscar S. Dalmau-Cedeño, Width attention based convolutional neural network for retinal vessel segmentation, Expert Syst. Appl. 209 (2022), 118313.

[138] Deng Xiangyu, Ye Jinhong, A retinal blood vessel segmentation based on improved D-MNet and pulse-coupled neural network, Biomed. Signal Process Control 73 (2022), 103467.
[139] Zheng Huang, Ming Sun, Yuxin Liu, Jiajun Wu, Csaunet, A cascade self-attention u-shaped network for precise fundus vessel segmentation, Biomed. Signal Process Control 75 (2022), 103613.
[140] Geetha Pavani, Birendra Biswal, Tapan Kumar Gandhi, Multistage Dpiref-Net, An effective network for semantic segmentation of arteries and veins from retinal surface, Neuroscience Informatics 2 (2022), 100074.
[141] Robert Arnar Karlsson, Sveinn Hakon Hardarson, Artery vein classification in fundus images using serially connected U-Nets, Comput. Methods Progr. Biomed. 216 (2022), 106650.
[142] D.A. Clevert, T. Unterthiner, S. Hochreiter, Fast and accurate deep network learning by exponential linear units (ELUs), 4th International Conference on Learning Representations, ICLR 2016 - Conference Track Proceedings (2016) 1–14.
[143] Zifan Zhu, An Qing, Zhicheng Wang, Li Qian, Hao Fang, Zhenghua Huang, Ilu-Net, Inception-Like U-Net for retinal vessel segmentation, Optik - International Journal for Light and Electron Optics 260 (2022), 169012.
[144] Pengshuai Yin, Hongmin Cai, Qingyao Wu, Df-Net, Deep fusion network for multi-source vessel segmentation, Inf. Fusion 78 (2022) 199–208.
[145] Tariq M. Khan, Syed S. Naqvi, Robles-Kelly Antonio, Imran Razzak, Retinal vessel segmentation via a Multi-resolution Contextual Network and adversarial learning, Neural Network. 165 (2023) 310–320.
[146] Renyuan Liu, Tong Wang, Xuejie Zhang, Xiaobing Zhou, DA-Res2UNet: Explainable blood vessel segmentation from fundus images, Alex. Eng. J. 68 (2023) 539–549.
[147] Meilin Liu, Zidong Wang, Li Han, Peishu Wu, Fuad E. Alsaadi, Nianyin Zeng, Aa-Wgan, Attention augmented Wasserstein generative adversarial network with application to fundus retinal vessel segmentation, Comput. Biol. Med. 158 (2023), 106874.
[148] K. He, G. Gkioxari, P. Dollár, R. Girshick, Mask r-cnn, in: Proceedings of the IEEE International Conference on Computer Vision, 2017, pp. 2961–2969.
[149] P. Liskowski, K. Krawiec, Segmenting retinal blood vessels with deep neural networks, IEEE Trans. Med. Imag. 35 (2016) 2369–2380, https://doi.org/10.1109/TMI.2016.2546227.
[150] Kyoung Jin Noh, Sang Jun Park, Soochahn Lee, Scale-space approximated convolutional neural networks for retinal vessel segmentation, Comput. Methods Progr. Biomed. 178 (2019) 237–246.
[151] K. Maninis, J. Pont-Tuset, P.A. Arbeláez, L.V. Gool, Deep retinal image understanding, in: Proc. Of Medical Image Computing and Computer Assisted Intervention, MICCAI), 2016, pp. 140–148, https://doi.org/10.1007/978-3-319-46723-8_17.
[152] Pearl Mary Samuel, Thanikaiselvan Veeramalai, VSSC Net, Vessel specific skip chain convolutional network for blood vessel segmentation, Comput. Methods Progr. Biomed. 198 (2021), 105769.
[153] K. Sun, B. Xiao, D. Liu, J. Wang, Deep High-Resolution Representation Learning for Human Pose Estimation, 2019, 09212 arXiv preprint arXiv:1902.
[154] A. Krizhevsky, I. Sutskever, G.E. Hinton, ImageNet classification with deep convolutional neural networks, Commun. ACM 60 (6) (2017) 84–90, https://doi.org/10.1145/3065386. May.
[155] Y. Liu, M.-M. Cheng, X. Hu, K. Wang, X. Bai, Richer convolutional features for edge detection, in: Proceedings of the IEEE Conference on Computer Vision and Pattern Recognition, 2017, pp. 5872–5881.
[156] I.J. Goodfellow, J. Pouget-Abadie, M. Mirza, B. Xu, D. Warde-Farley, S. Ozair, et al., Generative adversarial nets, in: Neural Information Processing Systems Conference, Canada, Montreal, Quebec, 2014.
[157] J. Dai, H. Qi, Y. Xiong, Y. Li, G. Zhang, H. Hu, Y. Wei, Deformable convolutional networks, in: International Conference on Computer Vision, 2017, pp. 764–773.
[158] Vijay Kendall Badrinarayanan, Cipolla Alex, Roberto, Segnet: a deep convolutional encoder-decoder architecture for image segmentation, IEEE Trans. Pattern Anal. Mach. Intell. 99 (2017), 1–1.
[159] H. Zhao, J. Shi, X. Qi, X. Wang, J. Jia, Pyramid scene parsing network, in: Proc IEEE Comput Soc Conf Comput Vision Pattern Recognit, 2017, pp. 2881–2890. Venice Italy.
[160] J. Staal, M.D. Abràmoff, M. Niemeijer, M.A. Viergever, B.V. Ginneken, Ridge-based vessel segmentation in color images of the retina, IEEE Trans. Med. Imag. 23 (4) (2004) 501–509.
[161] A. Hoover, M. Goldbaum, Locating the optic nerve in a retinal image using the fuzzy convergence of the blood vessels, IEEE Trans. Med. Imag. 22 (8) (2003) 951–958.
[162] Q. Li, B. Feng, L.P. Xie, P. Liang, H. Zhang, T. Wang, A cross-modality learning approach for vessel segmentation in retinal images, IEEE Trans. Med. Imag. 35 (2016) 109–118.
[163] J. Orlando, E. Prokofyeva, M. Blaschko, A discriminatively trained fully connected conditional random field model for blood vessel segmentation in fundus images, IEEE Trans. Biomed. Eng. 64 (2017) 16–27.
[164] L. Wang, H. Liu, Y. Lu, H. Chen, J. Zhang, J. Pu, A coarse-to-fine deep learn- ing framework for optic disc segmentation in fundus images, Biomed. Signal Process Control 51 (2019) 82–89.
[165] S. Abbasi-Sureshjani, I. Smit-Ockeloen, E. Bekkers, B. Dashtbozorg, B. ter Haar Romeny, Automatic detection of vascular bifurcations and crossings in retinal images using orientation scores, in: International Symposium on Biomedical Imaging (ISBI), IEEE, 2016, pp. 189–192.
[166] J. Orlando, H. Fu, J. Breda, K. Keer, D. Bathula, A. Pinto, R. Fang, P. Heng, J. Kim, J. Lee, J. Lee, X. Li, P. Liu, S. Lu, B. Murugesan, V. Naranjo, S. Phaye, S. Shankaranarayana, A. Sikka, J. Son, A. Hengel, S. Wang, J. Wu, Z. Wu, G. Xu, Y. Xu, P. Yin, F. Li, X. Zhang, Y. Xu, H. Bogunovic, REFUGE Challenge: a unified framework for evaluating automated methods for glaucoma assessment from fundus photographs, Med. Image Anal. 59 (2020), 101570.
[167] R.V.J.P.H. Kälviäinen , H. Uusitalo , Diaretdb1 diabetic retinopathy database and evaluation protocol, Med. Image Underst. Anal. 20 07 (20 07) 61.
[168] T. Kauppi, V. Kalesnykiene, J.K. Kamarainen, L. Lensu, I. Sorri, H. Uusitalo, H. Kälviäinen, J. Pietilä, Diaretdb0: Evaluation Database and Methodology for Diabetic Retinopathy Algorithms, Machine Vision and Pattern Recognition Re-Search Group vol. 73, Lappeenranta University of Technology, Finland, 2006.
[169] J. Sivaswamy, S. Krishnadas, A. Chakravarty, G. Joshi, A.S. Tabish, A comprehensive retinal image dataset for the assessment of glaucoma from the optic nerve head analysis, JSM Biomed Imaging Data Papers 2 (1) (2015) 1004.
[170] R. Wang, L. Zheng, C. Xiong, C. Qiu, H. Li, X. Hou, B. Sheng, P. Li, Q. Wu, Retinal optic disc localization using convergence tracking of blood vessels, Multimed. Tool. Appl. 76 (22) (2016) 1–23.
[171] F. Fumero, S. Alay′on, J.L. Sanchez, J. Sigut, M. Gonzalez-Hernandez, Rim-one: an open retinal image database for optic nerve evaluation, in: 24th International Symposium on Computer-Based Medical Systems, CBMS), 2011, pp. 1–6, 2011.
[172] M. Abdullah, M. Fraz, S. Barman, Localization and Segmentation of Optic Disc in Retinal Images Using Circular Hough Transform and Grow-Cut Algorithm, PeerJ, 2016.
[173] H. Kang, Y. Gao, S. Guo, X. Xu, T. Li, K. Wang, AVNet: a retinal artery/vein classification network with category-attention weighted fusion, Comput. Methods Progr. Biomed. 195 (2020), 105629.
[174] R. Estrada, C. Tomasi, S.C. Schmidler, S. Farsiu, Tree topology estimation, IEEE Trans. Pattern Anal. Mach. Intell. 37 (8) (2015) 1688–1701.
[175] H. Zhao, H. Li, S. Maurerstroh, L. Cheng, Synthesizing retinal and neuronal images with generative adversarial nets, Med. Image Anal. 49 (2018) 14–26.
[176] J.I. Orlando, J.B. Breda, K. Van Keer, M.B. Blaschko, P.J. Blanco, C.A. Bulant, Towards a glaucoma risk index based on simulated hemodynamics from fundus images, in: International Conference on Medical Image Computing and Computer-Assisted Intervention, Springer, 2018, pp. 65–73.
[177] A.A. Almazroa, S. Alodhayb, E. Osman, E. Ramadan, M. Hummadi, M. Dlaim, M. Alkatee, K. Raahemifar, V. Lakshminarayanan, Retinal Fundus Images for Glaucoma Analysis: the RIGA Dataset, 2018.
[178] L.M. Koesten, E. Kacprzak, J.F.A. Tennison, E. Simperl, The trials and tribulations of working with structured data: -a study on information seeking behavior, in: Proceedings of the 2017 CHI Conference on Human Factors in Computing Systems, ACM, New York, NY, USA, 2017, pp. 1277–1289, https://doi.org/10.1145/3025453.3025838.
[179] Tao Li, Bo Wang, Chunyu Hu, Hong Kang, Hanruo Liu, Kai Wang, Huazhu Fu, Applications of deep learning in fundus images: a review, Med. Image Anal. 69 (2021), 101971.
[180] Sourya Sengupta, Amitojdeep Singh, Henry A. Leopold, Tanmay Gulati, Vasudevan Lakshminarayanan, Ophthalmic diagnosis using deep learning with fundus images – a critical review, Artif. Intell. Med. 102 (2020), 101758.
[181] A.M. David, Y. Lou, E. Ali, C. Warren, A. Ryan, J.C. Folk, N. Meindert, Improved automated detection of diabetic retinopathy on a publicly available dataset through integration of deep learning, Invest. Ophthalmol. Vis. Sci. 57 (13) (2016) 5200.
[182] Jayaram K. Udupa, Dewey Odhner, Liming Zhao, Yubing Tong, M. Monica, S. Matsumoto, Krzysztof C. Ciesielski, Alexandre X. Falcao, Pavithra Vaideeswaran, Victoria Ciesielski, Babak Saboury, Syedmehrdad Mohammadianrasanani, Sanghun Sin, Raanan Arens, Drew A. Torigian, Body-wide hierarchical fuzzy modeling, recognition, and delineation of anatomy in medical images, Med. Image Anal. 18 (2014) 752–771.